

UNCLASSIFIED

AD NUMBER

ADA800031

CLASSIFICATION CHANGES

TO: unclassified

FROM: restricted

LIMITATION CHANGES

TO:
Approved for public release; distribution is unlimited.

FROM:
Distribution authorized to DoD only;
Administrative/Operational Use; 25 JAN 1952.
Other requests shall be referred to Bureau of
Ships, Washington, DC 20350. Pre-dates formal
DoD distribution statements. Treat as DoD only.

AUTHORITY

E.O. 10501 dtd 5 Nov 1953; USNSSC ltr dtd 7 Nov 1968

THIS PAGE IS UNCLASSIFIED

UNCLASSIFIED

DEFENSE DOCUMENTATION CENTER

SCIENTIFIC AND TECHNICAL INFORMATION

CAMERON, DON ALDRIA, VIRGINIA

CLASSIFICATION CHANGED
TO UNCLASSIFIED
FRC RESTRICTED

Classification changed in accordance with
Executive Order 10501 dated 5 November 1953
for the R. Danahy



UNCLASSIFIED

Reproduced by

DOCUMENT SERVICE CENTER

ARMED SERVICES TECHNICAL INFORMATION AGENCY

U. B. BUILDING, DAYTON, 2, OHIO

REL-C

721511

AMI

2053001

"NOTICE: When Government or other drawings, specifications or other data are used for any purpose other than in connection with a definitely related Government procurement operation, the U.S. Government thereby incurs no responsibility, nor any obligation whatsoever; and the fact that the Government may have formulated, furnished, or in any way supplied the said drawings, specifications or other data is not to be regarded by implication or otherwise as in any manner licensing the holder or any other person or corporation, or conveying any rights or permission to manufacture, use or sell any patented invention that may in any way be related thereto."

ATI No. 205300

STI

ASTIA FILE COPY

1579-41

A CLASS OF BROAD-BAND DISSIPATIVE
MATCHING NETWORKS DESIGNED ON
AN INSERTION - LOSS BASIS

by

Richard La Rosa

and

Herbert J. Carlin

RETURN TO:
ASTIA REFERENCE CENTER
LIBRARY OF CONGRESS
WASHINGTON 25, D.C.

NOTICE: THIS DOCUMENT CONTAINS INFORMATION AFFECTING THE NATIONAL DEFENSE OF THE UNITED STATES WITHIN THE MEANING OF THE ESPIONAGE LAWS, TITLE 18, U.S.C., SECTIONS 793 and 794. THE TRANSMISSION OR THE REVELATION OF ITS CONTENTS IN ANY MANNER TO AN UNAUTHORIZED PERSON IS PROHIBITED BY LAW.

PLEASE RETURN THIS COPY TO:

**ARMED SERVICES TECHNICAL INFORMATION AGENCY
DOCUMENT SERVICE CENTER
Knott Building, Dayton 2, Ohio**

Because of our limited supply you are requested to return this copy as soon as it has served your purposes so that it may be made available to others for reference use. Your cooperation will be appreciated.

RESTRICTED

Microwave Research Institute
Polytechnic Institute of Brooklyn
55 Johnson Street
Brooklyn 1, New York

Report R-264-52, PIB-203
Contract No. N0bsr-43360
Index No. NE-100-402

RUB

A CLASS OF BROAD-BAND DISSIPATIVE
MATCHING NETWORKS DESIGNED ON
AN INSERTION - LOSS BASIS

by
Richard La Rosa
and
Herbert J. Carlin

NAVY RESEARCH SECTION
SCIENCE DIVISION
LIBRARY OF CONGRESS
TO BE RETURNED

NAVY RESEARCH SECTION
SCIENCE DIVISION
REFERENCE DEPARTMENT
LIBRARY OF CONGRESS

MAR 17 1952

Title Page
Acknowledgment
Abstract
Table of Contents
26 Pages of Text
16 Pages of Figures
1 Page of References

copy # 81

Brooklyn 1, New York
January 25, 1952

SECURITY INFORMATION

RESTRICTED

RESTRICTED

Report R-264-52, PIB-203
Contract No. NObsr-43360
Index No. NE-100-402

ACKNOWLEDGMENT

Work covered by this report was sponsored
by the Navy, Bureau of Ships, under Contract
No. NObsr-43360.

RESTRICTED

RESTRICTED

Report R-264-52, PIB-203
Contract No. NObsr-43360
Index No. NE-100-402

ABSTRACT

The design of broad-band lossless matching networks is fairly well understood. Dissipative networks can perform functions which are not possible with lossless networks. The design of dissipative matching networks which dissipate a minimum of power is neither straightforward nor completely understood at present. Various types of networks are discussed and numerical designs are carried out for specific cases.

RESTRICTED

RESTRICTED

Report R-264-52, PIB-203
Contract No. NObsr-43360
Index No. NE-100-402

TABLE OF CONTENTS

	<u>Page No.</u>
Acknowledgment	
Abstract	
I. The Application of Dissipative Matching Networks.	1
II. Properties of Matching 4-poles.	2
A. Specification of the Matching Problem.	2
B. Network Equations of Matching 4-poles.	3
C. Realizability of Matching Networks Without Regard to Insertion Loss.	4
III. Some Matching Structures.	5
A. Matching Procedures for the load $z = 1 + pL_0$.	5
B. Complementary Filters as Matching Networks.	6
C. An L-section Matching Network.	13
1. Design Objective.	13
2. Graphical Calculation of $z_1(j\omega)$.	15
3. Specification of Impedance Locus.	16
4. Sample Calculation.	17
5. Integral Formula Calculation of Cutoff Frequency.	18
6. Performance of Series-L Matching Network.	21
D. The Shunt-L Matching Network.	21
E. A T-pad Matching Network.	24
IV. Comparison of Various Matching Networks.	25

RESTRICTED

I. The Application of Dissipative Matching Networks

In designing microwave equipment, it is often necessary to match the input impedance of some component to a resistive generator or to the characteristic impedance of a lossless line. When this match is required over a narrow band, a pair of reactive elements, (stubs, tuning screws, etc.) or a single element placed at a particular point on the line, can be used to give a perfect match at the mid-frequency. The mismatch at the edges of the band may be small enough (because of the narrowness of the band) so that a "single-frequency" match is adequate. When the load which is to be matched has an impedance which varies slowly as a function of frequency, tuning elements which store a minimum amount of energy are used in order to obtain the greatest bandwidth. When the load has some particular change with frequency, it is possible to pick tuning elements whose reactance change with frequency compensates for the load impedance change and thus gives a satisfactory match over a band.

The simple procedure outlined above is adequate for many situations encountered in the design of radars, communication facilities, and some narrow band test equipment. When antennas are connected to transmitters by long transmission lines, it is often necessary to match more carefully to avoid frequency pulling. In this case, more effort is expended in the choice of line lengths, transformers and stubs in order to give as nearly perfect match as possible in the transmitter band.

The above remarks apply to problems where simple lossless elements are adequate to give the required match. As the maximum permitted VSWR becomes smaller, or the required bandwidth becomes greater, the design becomes more difficult. Eventually, a point is reached when it is impossible to obtain required performance. When lossless matching networks are used, it is not possible, with physical elements, to match perfectly over any finite bandwidth. The question of what amount of mismatch must be tolerated for a particular load impedance and specified frequency band has been treated by R. M. Fano.⁽¹⁾

When the required performance is greater than the possible limit for lossless matching networks, it is necessary to include dissipative elements in the matching network. One simple method of doing this is known as "padding". A dissipative attenuator can be placed in front of the load and if the attenuation is great enough, the input impedance of the attenuator can be matched to the generator or transmission line. This is a common procedure because (1) there may be more than sufficient power available and (2) broadband matched attenuators are usually available. This process is not good when signal strength is at a premium.

RESTRICTED

Report R-264-52. PIB-203
Contract No. NObsr-43360
Index No. NE-100-402

Page 2

because it is wasteful of power. It simply consists of putting in enough insertion loss so that the load cannot be "seen" from the input terminals of the matching or so-called buffer attenuator. It is therefore desirable to investigate matching networks which include dissipative elements which are inserted in such a way that power waste is minimized.

II Properties of Matching 4-poles

A. Specification of the Matching Problem

A load is given which has an impedance $Z(p)$ where $p = \sigma + j\omega$ is the complex frequency variable. Power is supplied by a generator whose internal resistance is R_0 . A lossy four-terminal network (4-pole) is connected between generator and load as in Fig. MRI-11968-a. The matching network is to be composed of linear, passive elements and should do the following:

(a) The input impedance of the load and matching network, i.e., the impedance presented to the generator, should be constant and equal to R_0 for all values of p .

(b) In a specified range of sinusoidal frequencies ($\sigma = 0$, $0 \leq \omega \leq \omega_c$), the power in the load should be constant to within a certain tolerance and this constant should be as large as possible.

The above requirements are more restrictive than would be desirable in many practical problems, but they provide sufficient latitude for the present study. Note that although low-pass performance is usually not desirable in microwave work, many loads encountered in practice have geometric symmetry about some center frequency. These loads have low-pass equivalents: knowledge obtained for the low-pass problem can be applied to them. Results of the present investigation can also be extended by means of high-pass transformations.

In what follows, all impedances are normalized to R_0 so that the generator has a one ohm internal impedance, and the load is $z(p) =$

$\frac{Z(p)}{R_0}$. The open circuit voltage of the generator is arbitrarily fixed at 2 volts (RMS) so that the available power from the generator is 1 watt.

The power that is dissipated in the load is of physical significance only when $\sigma = 0$, since the $j\omega$ axis of the p -plane corresponds to sinusoidal frequencies (steady-state a.c.). This power is

RESTRICTED

RESTRICTED

Report R-264-52, PIB-203
Contract No. NObSr-43360
Index No. NE-100-402

Page 3

written as a function of ω and is written $P(\omega)$. $P(\omega)$ is the actual power in watts for the normalized system. $P(\omega)$ is identically the ratio of power dissipated in the load to the available power of the generator. Note that the power entering the input terminal of the 4-pole is the available power of the generator (because it is perfectly matched). Therefore, $P(\omega)$ can also be interpreted as the ratio of power leaving the output terminals of the matching network to the power entering the input terminal of the matching 4-pole.

B. Network Equations of Matching Four-Poles

The 4-pole is characterized by three parameters, $z_{11}(p)$, $z_{22}(p)$, $z_{12}(p)$ which are the open circuit input, output, and transfer impedances, respectively. When the 4-pole is terminated in z , its input impedance is:

$$z_{in} = z_{11} - \frac{z_{12}^2}{z_{22} + z} \quad (1)$$

$z_{in} = 1$ to satisfy requirement (a) of Part II A so that the three parameters are related by the following equations:

$$z_{11} = 1 + \frac{z_{12}^2}{z_{22} + z} \quad (2a)$$

$$z_{12}^2 = (z_{11} - 1)(z_{22} + z) \quad (2b)$$

If $z(p=j\omega) = r(\omega) + jx(\omega)$: the expression for $P(\omega)$ is:

$$P(\omega) = \left| \frac{z_{12}}{z_{22} + z} \right|^2 r(\omega) = \left| \frac{z_{11} - 1}{z_{22} + z} \right|^2 r(\omega) \quad (3)$$

Thus, there are two general relations; one of them (Equations 2a, 2b) is algebraic, but the other one (Equation 3) involves magnitudes of sums of impedances and the real part of $z(j\omega)$. One of the 4-pole parameters can be arbitrarily picked because there are only two relations. It is important to note that this arbitrary parameter is a function of the complex variable p .

One additional consideration makes the problem extremely difficult. The 4-pole must be physically realizable as a linear, passive network. Whether it is composed of lumped inductance, capacitance, and

resistance, or distributed elements is a question that need not be considered here. In some of the examples that will be discussed, the matching network will be composed of lumped elements, while in others, various impedances will be given as empirically determined functions of ω , and therefore might be synthesized by either lumped or distributed elements.

One ideal transformer will be allowed in the matching network, either at the output or input end. This avoids complication in the treatment of the problem and is justified in practice because,

(a) -- There is often considerable choice of impedance level at the terminals of a microwave load (where to tap into a cavity for instance). This freedom of choice corresponds to the availability of an ideal transformer.

(b) When sufficient physical space is available, an ideal transformer at the input of the matching network can be simulated by a long tapered transmission line. Note that if long lines are employed they must be put at the input of the matching network, for the input impedance of a long line terminated in a mismatched load is a complicated function of frequency and is difficult to match.

C. Realizability of Matching Networks without Regard to Insertion Loss

Given any realizable load function $z(p)$, it is always possible to provide a 4-pole which will, when terminated in $z(p)$ have unit input impedance. To show this, a simple method of matching will be described which makes use of the following theorem:

If $Z_1(p)$ is a physically realizable minimum reactance impedance (i.e. $Z_1(p)$ has no pole on the $j\omega$ axis of the p -plane), it is possible to find a $Z_2(p)$ such that

$$Z_1(p) + Z_2(p) = R \quad (4)$$

If $Z_1(j\omega) = R_1(\omega) + jX_1(\omega)$, then

$$R \geq \text{maximum value of } R_1(\omega) \quad (5)$$

The proof of this theorem is given by Bode⁽²⁾.

Applying this to a given minimum reactance load $z(p)$, it is clear that if the real part of $z(p)$ along $j\omega$ obeys:

$$\text{maximum } r(\omega) \leq 1 \quad (6)$$

then a two-terminal impedance connected in series with the load can be designed to give a perfect match to a 1 ohm generator.

If $\text{Max } r(\omega) > 1$, a transformer can precede or follow the series matching impedance to adjust the impedance level to the unit value required.

If $z(p)$ is not minimum reactance, a new $z'(p)$ function can be formed by placing a resistor of any value in parallel with $z(p)$. This new $z'(p)$ function will then be minimum reactance and an impedance, $z_1(p)$ can be put in series with $z'(p)$ to give a perfect match to some constant resistance. This constant resistance can be transformed to unity as before by means of an ideal transformer.

III. Some Matching Structures

A. Matching Procedures for the load $z = 1 + pL_0$

As shown in Section II C, it is always possible to match any load, $Z(p)$, to a 1 ohm generator by means of a realizable dissipative 4-pole. The problem to be considered here is to find the network which gives the greatest transfer of power to the load in a prescribed frequency band. In the beginning of this investigation, an attempt was made to discover some explicit expression of the constraints, such as integral formulas, which would show the limitations imposed on $P(\omega)$ by the specification of the bandwidth and the load $Z(p)$. It seemed that a treatment of lossy structures similar to that given by Fano⁽¹⁾ for lossless structures would give similar results, i.e., the integral of some function of $P(\omega)$ on some frequency scale would be related to properties of the load. No such relations were found, however: either significant integrals did not converge, or convergent integrals were not significant. This was a manifestation of a fundamental property possessed by a lossless 4-pole but not possessed by a lossy 4-pole. If a number of lossless 4-poles are connected in tandem and the reflection coefficient $\rho(\omega)$ at any pair of terminals is defined according to Bode⁽³⁾ as:

$$\rho = \frac{\text{impedance looking to left} - \text{conjugate of impedance looking to right}}{\text{impedance looking to left} + \text{impedance looking to right}} \quad (7)$$

Report R-264-52, PIB-203
 Contract No. NObser-43360
 Index No. NE-100-402

then $|\rho|$ is the same at any pair of terminals from the input of the lossless chain to the output of the lossless chain. The load may be represented by Darlington's procedure⁴ as a lossless 4-pole terminated in a 1 ohm resistor. The 4-pole and the lossless matching network form a chain of 2 lossless networks as shown in Fig. MRI-12339-a. For some values of p there is no transmission through the 4-pole (N') which characterizes the load. The function $\log \rho_2$ can be expanded in a Taylor series about one of these values of p . At those values of p which are in the right-hand half-plane or on the $j\omega$ axis, a certain number of coefficients in the Taylor expansion are determined entirely by the given load. Integral formulae are then obtained relating $\log |\rho_2|$ to the known Taylor coefficients in the expansion ρ_2 . But since $|\rho_1| = |\rho_2|$, the same relation applies to $|\rho_1|$ which is the input reflection coefficient. $|\rho_1|$ is of direct significance since it determines the VSWR of the matched load.

The immediate study of the general load cannot proceed much further, however, because there has not been sufficient study of the properties of a dissipative 4-pole. For this reason, the scope of the investigation has been limited for the present by the following two restrictions:

(1) A particular load function is studied, $z(p) = 1 + pL_0$

(2) Particular forms of matching structures are studied.

These have properties which simplify analysis. By means of frequency transformations, the results obtained can be extended to band-pass performance with a series R-L-C load and high pass performance with a series R-C load.

By interchanging admittance and impedance, the results can be applied to the low-pass performance of parallel G-C, bandpass performance of parallel G-L-C and high-pass performance of parallel L-G loads.

The two band-pass cases mentioned above are often encountered in practical microwave loads such as resonant cavities and antennas.

B. Complementary Filters as Matching Networks

The matching devices to be described here are to be associated with the load $z(p) = 1 + pL_0$ and make use of some ideas of E. L. Norton⁵ and H. W. Bode⁶. In this section, let $\omega_c = 1$. This is no restriction

Report R-264-52, PIB-203
 Contract No. NObsr-43360
 Index No. NE-100-402

because the parasitic inductance L_0 of the load is not fixed. Changing the value of L_0 is equivalent to changing the frequency scale, or, equivalently, the bandwidth of interest.

These matching structures are in the forms of Fig. MRI-11968-b and Fig. MRI-11968-c. The lossless networks shown in these figures are used to modify the normalized resistance r_1 and normalized conductance g_1 to approximate unity over the band $0 \leq \omega \leq 1$. "Minimum reactance input" and "minimum susceptance input" refer to the input impedance of the lossless network when terminated in the load $1 + jL_0$.

Note that when the input of the lossless network is of minimum reactance type an impedance is placed in series; when the input is minimum susceptance, an admittance is placed in shunt. As long as the resistance r_1 or the conductance g_1 is less than 1, the lossy 2-poles are physically realizable.

The normalized current into the lossless network of Fig. MRI-11968-b is constant and unity. The normalized voltage across the input of the lossless network of Fig. MRI-11968-c is constant and unity. Therefore:

$$P(\omega) = \begin{cases} r_1(\omega) & \text{in Fig. MRI-11968-b} \\ g_1(\omega) & \text{in Fig. MRI-11968-c} \end{cases} \quad (8)$$

Low pass ladder structures of Fig. MRI-12341-a and Fig. MRI-12341-b are used in this case as the lossless networks which shape $r_1(\omega)$ and $g_1(\omega)$ into Butterworth and Tschebycheff approximations of unity. The ideal transformers at the ladder inputs are used to adjust the impedance levels so that r_1 (or g_1 when applicable) is never greater than 1. $P(\omega)$ is restricted to the following range:

$$\frac{1}{1 + \epsilon^2} \leq P(\omega) \leq 1 \quad \text{for } 0 \leq \omega \leq \omega_c \quad (9)$$

The ideal transformer ratio N is picked so that $\max P(\omega) = 1$. This is equivalent to saying that $\max r_1(\omega) = 1$ (or $\max g_1 = 1$). The ratio N is equal to 1 in most of the filters to be discussed here; only for the even order Tschebycheff functions is $N \neq 1$.

RESTRICTED

Report R-264-52, PIB-203
 Contract No. NObsr-43360
 Index No. NE-100-402

Page 8

For the load $z(p) = 1 + pL_0$, we know that

$$\lim_{\omega \rightarrow \infty} P(\omega) = 0 \quad (10)$$

because an open circuit cannot absorb power from a generator whose impedance and open circuit voltage are finite.

The Butterworth function which satisfied Eq. (9) and Eq. (10) is:

$$P(\omega) = \frac{1}{1 + \epsilon^2 \omega^{2n}} \quad (11)$$

In what follows, it is necessary to introduce a quantity $P'(p)$ which is a function of the complex variable $p = \sigma + j\omega$. When $\sigma = 0$, $P'(0 + j\omega)$ is real and is equal to $P(\omega)$ which is the power in the load. Thus $P'(p)$ is the analytic continuation of the function $P(\omega)$ which is defined in Eq. (11) only for real values of ω .

$$P'(p) = \frac{1}{1 + \epsilon^2 \left(\frac{p}{J}\right)^{2n}} = \frac{1}{J^{2n} \prod_{l=1}^n (p - p_l) \prod_{l=1}^n (p + p_l)} \quad (12)$$

where J is a real constant.

The Tschebycheff approximation satisfying Eq. (9) and Eq. (10) is:

$$P(\omega) = \frac{1}{1 + \epsilon^2 T_n^2(\omega)} \quad (13)$$

$$P'(p) = \frac{1}{1 + \epsilon^2 T_n^2\left(\frac{p}{J}\right)} = \frac{1}{J^{2n} \prod_{l=1}^n (p - p_l) \prod_{l=1}^n (p + p_l)} \quad (14)$$

The factored forms of Eq. (14) and Eq. (12) may be interpreted with the aid of Fig. MRI-12342 and Fig. MRI-119, 1 which show the location of poles $P(p)$. The $2n$ roots are symmetrically disposed about both axes, so that

$$\prod_{l=1}^n (p - p_l)$$

contains all the roots in the L. H. p-plane and

$$\prod_1^n (p + p_j)$$

contains all the roots in the R.H. p-plane. Note that no roots occur on $\sigma = 0$.

If a_1, a_2, b_1, b_2 are even polynomials in p with positive real coefficients.

$$\frac{z_{12}}{z_{22} + z} = \frac{a_1 + p b_1}{a_2 + p b_2} \quad (15)$$

$$P(p) = \frac{a_1^2 - p^2 b_1^2}{a_2^2 - p^2 b_2^2} \quad (16)$$

Eq. (16) may be checked by noting that for $\sigma = 0$

$$P^1(j\omega) = P(\omega) = \frac{a_1^2 + \omega^2 b_1^2}{a_2^2 + \omega^2 b_2^2} = \frac{|a_1 + j\omega b_1|^2}{|a_2 + j\omega b_2|^2} = \left| \frac{z_{12}}{z_{22} + z} \right|^2 \quad (17)$$

which agrees with Eq. (3) because $r(\omega) = 1$.

The relation between tolerance ϵ^2 and parasitic load inductance L_0 may be found by writing Eq. (16) as the product of a factor containing poles in L.H. p-plane and a factor containing poles in R.H. p-plane. The two highest power terms in the L.H. p-plane expression are related to L_0 . To show this, L_0 has been combined (Figs. MRI-12341-c and MRI-12341-d) with the lossless ladders to give ladders having the parameters z_{11}, z_{12}, z_{22} . These are fed by unit generators and terminated in the unit resistor of the load.

$$z_{22} = \frac{a}{p b} = \frac{a_{2k} p^{2k} + a_{2k-2} p^{2k-2} + \dots + a_0}{p [b_{2k-2} p^{2k-2} + \dots + b_0]} \quad (18)$$

$$z_{12}^i = \frac{a_0}{pb} \quad (19)$$

The a_0 of (18) and (19) are identical. For the networks of Fig. MRI-12341-c and Fig. MRI-12341-d,

$$\frac{z_{12}^i}{z_{22}^i + 1} = \frac{a_0}{a + pb} \quad (20)$$

$$P'(p) = \frac{a_0^2}{a^2 - p^2 b^2} = \frac{a_0^2}{(a + pb)(a - pb)} \quad (21)$$

It can be shown that because a/pb is a physically realizable reactance function, $(a + pb)$ has roots only in the L.H. p -plane and $(a - pb)$ has roots only in the R.H. p -plane. Therefore $a + pb$ can be compared with $\prod_{1}^n (p - p_{\nu})$

$$\begin{aligned} a + pb &= (a_{2k} p^{2k} + \dots + a_0) + p (b_{2k-2} p^{2k-2} + \dots + b_0) \\ &= a_{2k} \prod_{1}^n (p - p_{\nu}) = a_{2k} (p^{2k} - p^{2k-1} \sum_{1}^n p_{\nu} + \dots) \end{aligned} \quad (22)$$

$$\frac{b_{2k-2}}{a_{2k}} = - \sum_{1}^n p_{\nu} \quad (23)$$

But from the z_{22}^i expression

$$L_0 = \frac{a_{2k}}{b_{2k-2}} = \frac{-1}{\sum_{1}^n p_{\nu}} \quad (24)$$

The roots are a function of ϵ and n ; therefore L_0 can be found from ϵ and n . Because the roots are symmetrically disposed about the σ axis, only the sum of the real parts need be taken. This has been

indicated by the heavy lines in Figs. MRI-12342 and MRI-11971. Since the real parts are all negative,

$$L_0 = \left| \frac{1}{\sum_1^n R_e p_j} \right| \quad (25)$$

Using the relation

$$\sum_1^n \sin (2k-1) \frac{\pi}{2n} = \frac{1}{\sin \frac{\pi}{2n}} \quad (26)$$

The relation between ϵ and L_0 for the Butterworth case (Fig. MRI-12341) is

$$L_0 = \frac{1}{\sum_1^n \sin (2k-1) \frac{\pi}{2n}} = \sin \frac{\pi}{2n} \quad (27)$$

$$L_0 = \sin \frac{\pi}{2n} \quad (28)$$

and for

$$n \gg 1 \quad L_0 \approx \frac{\pi}{2n} \quad (29)$$

For the Tschebycheff case (Fig. MRI-11971)

$$L_0 = \frac{1}{\sinh a \sum_1^n \sin (2k-1) \frac{\pi}{2n}} = \frac{\sin \frac{\pi}{2n}}{\sinh a} \quad (30)$$

where $\frac{1}{\epsilon} = \sinh n a$

For $n \gg 1$ and L_0 non-zero, $\sinh a \approx a$,

$$\sin \frac{\pi}{2n} \approx \frac{\pi}{2n}, \text{ and } L_0 \approx \frac{\pi}{2n\epsilon}$$

so that

$$\frac{1}{\epsilon} \approx \sinh \frac{\pi}{2L_0} \quad (31)$$

The results for the Tschebycheff and Butterworth networks are quite different: for the Butterworth, $P(\omega)$ can approach a rectangular shape as n gets large, but L_0 must approach zero; or equivalently, the actual bandwidth in cycles approaches zero for fixed L_0 . This is illustrated in Fig. MRI-11972-a where L_0 is decreased as n is increased in order to maintain bandwidth. As the curve approaches a rectangular form, the specification of tolerance, ϵ , becomes of decreasing importance because the curve becomes very steep at $\omega = 1$ and the actual ordinate at $\omega = 1$ may vary from 0 to 1 with a negligible change in cut-off frequency. For this reason ϵ drops out of the approximate relation Eq. (29). Fig. MRI-11972-a also illustrates the fact that over a restricted range of L_0 and ϵ , using a larger value of n may allow an increase in L_0 for fixed ϵ or a decrease in ϵ for fixed L_0 . Notice that for the value of ϵ used, a larger value of L_0 was permitted for $n = 2$ than for $n = 1$. $n = 3$ permitted a much lower value of L_0 , however. The curves of Fig. MRI-11972-b show that it is possible to improve performance by increasing n only for small values of ϵ and L_0 .

In the Tschebycheff design, L_0 need not approach zero as n increases. However, nature is not making much of a concession here because ϵ very quickly approaches a limit as n increases. Making n greater than 3 sharpens the cutoff and increases the number of ripples in the pass band, but the ripple amplitude does not decrease significantly. This is sketched in Fig. MRI-11972-c.

For large L_0 ($L_0 \gg 3$) the approximate relation Eq. (31) becomes

$$\epsilon = \frac{2}{\pi} L_0 \quad (32)$$

This means that the $P(\omega)$ curve looks like a series of narrow spikes. This is not a desirable type of response. A more useful type of equal-ripple response would sacrifice some gain at the peaks in return for greater flatness. This is not possible with the low-pass lossless ladders shown.

In summary, by assuming a simple form of the matching network and simple approximating functions for $P(\omega)$ it has been possible to relate $P(\omega)$ curves to the parasitic load inductance L_0 . Choice of the approximating function completely fixes the parameters of the lossless ladder. This determines the normalized impedance z_1 (or admittance y_1) at the ladder input. The 2-pole is a lossy network having impedance $1 - z_1$ (or admittance $1 - y_1$) and may be synthesized by standard procedure. The 2-pole, incidently, is the other filter in the "complementary filter" matching scheme.

If $n = 1$, the lossless networks of Fig. MRI-11968-b and MRI-11968-c reduce to mere straight-through connections. Then the input of the lossless network is minimum susceptance and Fig. MRI-11968-c is used. The lossy 2-pole consists of the resistor and capacitor in series of Fig. MRI-12339-b where the capacitor had the same numerical value (in farads) as the inductor (in henries).

Note that the approximating functions used here make $P(\omega) = 1$ at one or more values of ω . It would be desirable to have a $P(\omega)$ which is more uniform in the pass-band. That is, increase the minima at the expense of the maxima, or, better still, use a larger value of L_0 with less ripple than that allowed in the above Tschebycheff expansion for instance. In short, reduce the maxima of $P(\omega)$ in exchange for the improvement of some other characteristic of $P(\omega)$, as illustrated by the change from Fig. MRI-12339-c to Fig. MRI-12339-d.

From Eq. (8) it can be seen that reducing the maximum of $P(\omega)$ merely means reducing the maximum of $r_1(\omega)$ or $g_1(\omega)$. But there is no significance to reducing all these maxima because the ideal transformer at the input of the ladder can always be adjusted to make the maximum $r_1(\omega)$ or $g_1(\omega) = 1$. Thus, $P(\omega)$ should be equal to 1 for at least one value of ω , no matter what shape $P(\omega)$ may have, as illustrated by Fig. MRI-12339-e. This indicates that the complementary filter type of matching structure does not allow complete freedom in exchanging one characteristic of $P(\omega)$ for an increase in another characteristic which may be more desirable. Therefore, it may be profitable to devise a matching structure in which all maxima of $P(\omega)$ can be made less than unity in order to obtain increased bandwidth or greater allowable L_0 for the same ripple.

C. An L-section Matching Network.

1. Design Objective

In this section, the simple L-section and ideal transformer of Fig. MRI - 12300-a will be used to match the load $1 + pL_0$.

At the outset, L_0 is set equal to 1, and ω_c is considered as an index of performance to be determined. This corresponds to normalizing the complex frequency variable $p = \sigma + j\omega$ to the value $\frac{1}{L_0}$. This normalization is better adapted to the procedure which will follow. As in part B, no loss of generality results.

The object of the design is to obtain (in addition to matching the generator perfectly at all frequencies) a curve of normalized power in the load $P(\omega)$ which is flat for all ω from zero to some cutoff frequency ω_c . The value of ω_c should be as large as possible consistent with the value of P_0 chosen for $P(\omega)$ in the range of interest. $P(\omega)$ for $\omega > \omega_c$ is of no interest in this problem.

The problem, as stated, resolves itself into the determination of the value of ω_c corresponds to each choice of P_0 ; that is, P_0 is chosen as a parameter and then physically realizable 2-terminal impedances z_1 and z_2 are found which make $P(\omega) = P_0$ up to the largest possible value of ω_c .

Examination of the R.M.S. voltages marked in Fig. MRI-12300-a will show that

$$P(\omega) = \frac{2}{|1 + j\omega + z_1(j\omega)|^2} \quad (33)$$

In order to obtain a perfect match

$$y_3(p) = \frac{1}{1 + p + z_1(p)} \quad (34)$$

In order for $y_3(p)$ to be physically realizable

$$\frac{1}{n^2} \geq \text{max real part of } \frac{1}{1 + j\omega + z_1(j\omega)} \quad (35)$$

If the imaginary part of $1 + j\omega + z_1(j\omega)$ is plotted against the real part as a parametric function of ω it can be seen that in order to make $P(\omega) = P_0$, the locus of $1 + j\omega + z_1(j\omega)$ should follow a circular arc centered about the origin of the z -plane for $0 \leq \omega \leq \omega_c$. This is curve 1 of Fig. MRI-12134. At $\omega = 0$, any impedance is real and therefore the arc crosses the real axis at $\omega = 0$. The circle 1 is drawn in both

directions from the $\omega = 0$ point because there is, so far, no knowledge of what frequency scales are possible along the locus. The desired circular arc in the s -plane of Fig. MRI-12134 maps into the circular arc 1 of the y -plane. It is seen that the maximum conductance of this locus occurs at the point corresponding to $\omega = 0$. This d.c. conductance sets the maximum value of ideal transformer ratio n , provided the uncontrolled ($\omega > \omega_c$) part of the $1/1 + j\omega + z_1(j\omega)$ locus does not cut into the shaded region of the y -plane.

This forbidden region of the y -plane maps into the shaded circular area of the z -plane. The locus of $1 + j\omega + z_1(j\omega)$ should not pass into this forbidden circle. In addition, the real part of $z_1(j\omega)$, $r_1(\omega)$, should not be negative. Therefore, the locus $1 + j\omega + z_1(j\omega)$ should not enter the shaded region to the left of the line $\sigma = -1$.

The choice of P_0 corresponds to picking a value of r_0 , the radius of the desired arc in the z -plane. This makes

$$n^2 = r_0 \quad (36a)$$

$$P_0 = \frac{n^2}{|1 + z_1(0)|^2} = \frac{r_0}{r_0^2} = \frac{1}{r_0} \quad (36b)$$

2. Graphical Calculation of $z_1(j\omega)$

The value of ω_c corresponding to a particular r_0 is determined by finding an impedance $z_1(p)$ which makes the locus of $1 + j\omega + z_1(j\omega)$ follow the circular arc of radius r_0 . This can be done by trial and error with the aid of charts in "Network Analysis and Feedback Amplifier Design", H. W. Bode, Van Nostrand, 1945, Chapter 15 and with the aid of tables in "Phase of a Semi-Infinite Unit Attenuation Slope", D. E. Thomas, Bell Telephone System Monograph B-1511. The trial and error procedure is as follows:

- (1) Arbitrarily pick a curve $r_1(\omega)$.
- (2) Assuming that $z_1(p)$ is a minimum reactance function, use the numerical charts and tables to compute $x_1(\omega)$.
- (3) Plot the locus $1 + r_1(\omega) + j\omega + jx_1(\omega)$.
- (4) Make corrections in the $r_1(\omega)$ curve to make the locus follow more closely the desired circular arc.

The above procedure amounts to little more than picking $r_1(\omega)$ curves "out of the hat". Two steps are necessary in order to obtain an answer by this procedure:

- (1) The exact locus of $1 + j\omega + z_1(j\omega)$ must be specified. Until now, the only specification has been that it should follow the circular arc of radius r_0 for as large a frequency range as possible and should not go through certain forbidden regions.
- (2) A type of elementary resistance function should be chosen which will permit a reasonably systematic, convergent building-up of the desired $r_1(\omega)$ function from the elementary resistance functions.

3. Specification of Impedance Locus

The following conclusions are supported by various amounts of rigorous proof:

- (a) $z_1(p)$ should be a minimum reactance function. A pole at $p = \infty$ would be equivalent to adding parasitic inductance to the given load; this is clearly undesirable. A pole in the range $0 < \omega < \omega_c$ is not allowed because $P(\omega)$ must have a zero whenever $1 + p + z_1(p)$ has a pole on the $p = j\omega$ axis. The only other possible way for $z_1(p)$ to be non-minimum-reactance is for it to have a pole on the finite $j\omega$ axis at a frequency greater than ω_c . But the effect of such a pole on the properties of $z_1(j\omega)$ in the passband would be similar to the effect of a pole at infinity. The indication is, therefore, that $z_1(p)$ should be minimum reactance.
- (b) $r_1(\omega) = 0$ for $\omega > \omega_c$. Area under the resistance curve at frequencies above the pass band adds, in the pass band, positive reactance which varies linearly at low frequencies and increases slope as the cutoff frequency is approached. Within the pass band, the shape of this reactance curve

cannot be closely controlled because the resistance area which produces the reactance is outside of the pass band. Thus, resistance area above the pass band is equivalent to additional parasitic inductance in the load, and is undesirable. Therefore the $1 + j\omega + z_1(j\omega)$ locus should meet the $r = 1$ line when $\omega = \omega_c$ and must lie on this line for all $\omega > \omega_c$.

- (c) Experience with a large number of loci seems to indicate that after $1 + j\omega + z_1(j\omega)$ meets the $r = 1$ line at $\omega = \omega_c$, the tracing point cannot move down the $r = 1$ line and then reverse its direction and move back up; it apparently always moves in an upward direction, approaching the impedance $1 + j\omega$ at large ω . This, incidentally, insures that the locus will not cut into the shaded circle of Fig. MRI-12134.

As a result of these considerations it may be concluded that the ideal impedance locus is of the form shown in Fig. MRI-12340-a.

4. Sample Calculation

The elementary resistance function which was found to be most useful in building up the $r_1(\omega)$ curve is shown in Fig. MRI-12340-b. Charts of reactance corresponding to this "finite line segment" resistance curve are given in Bode, Chapter 15.

Several $r_1(\omega)$ curves and their corresponding $1 + j\omega + z_1(j\omega)$ loci are shown in Fig. MRI-12136 and Fig. MRI-12137. These are some of the curves obtained in the successive approximation solution for $r_0 = 2$. Note that in the first two curves, the value picked for ω_c is too low and the calculation curve goes inside of the desired contour. In the last two, the value of ω_c is about right and the calculated curve is almost equally distributed about the desired arc. Thus, $\omega_c = 2.6$ for $r_0 = 2$. It might be suspected that if the $r_1(\omega)$ curve were refined to obtain a closer approximation to the circular locus, the frequency scale might be changed considerably and, therefore, 2.6 is not very close to the correct value of ω_c . That this is not true can be shown by the following integral calculation.

5. Integral Formula Calculation of Cutoff Frequency

The complex transmission coefficient $t(p)$ is shown in Fig. MRI-12300-a as the complex voltage across the load resistor when the excitation is as shown in the figure. $t(p)$ is seen to be

$$t(p) = \frac{n}{1 + p + z_1(p)} \quad (37)$$

Making $P(\omega)$ flat for $0 \leq \omega < \omega_c$ corresponds to making $|t(j\omega)|$ flat over the same range. Call this value t_0 . The behavior for large p is determined by the parasitic unit inductance (since z_1 is a minimum reactance function) so that

$$\lim_{p \rightarrow \infty} t(p) = \frac{n}{p} \quad (38)$$

The following line integral taken around the p -plane path of Fig. MRI-12340-c encloses no poles and hence is zero. In addition, the closure along the infinite arc contributes nothing to the integral.

$$\oint \frac{\log \frac{n}{p} - \log t}{\sqrt{1 + \left(\frac{p}{\omega_c}\right)^2}} dp = 0 \quad (39)$$

and taking into account the oddness and evenness of the amplitude and phase of the integrand of Eq. (39) along $j\omega$, one obtains

$$\int_0^{\omega_c} \frac{\log \frac{n}{\omega} - \log |t|}{\sqrt{1 - \left(\frac{\omega}{\omega_c}\right)^2}} d\omega = \int_0^{\omega_c} \frac{\left(\frac{\pi}{2} + \theta\right) d\omega}{\sqrt{\left(\frac{\omega}{\omega_c}\right)^2 - 1}} \quad (40)$$

where θ is defined by:

$$t = |t| e^{j\theta} \quad (41)$$

The left hand side of Eq. (40) becomes a simple integration on a sinusoidal frequency scale if $\omega/\omega_c = \sin \phi$. The right hand side

can be transformed by letting $\sec \nu = \omega/\omega_c$. Eq. (40) becomes:

$$\int_0^{\omega_c} \frac{\log \frac{n}{\omega}}{\sqrt{1 - (\frac{\omega}{\omega_c})^2}} \frac{d\omega}{\omega_c} = \int_0^{\pi/2} \log |t| d\theta = \int_0^{\pi/2} (\theta + \frac{\pi}{2}) \sec \nu d\nu \quad (42)$$

The first integral is easily evaluated by No. 513 of Pierce's Tables. Its value is

$$\frac{\pi}{2} \log 2 - \frac{\pi}{2} \log \frac{\omega_c}{n} \quad (43)$$

The second integral is evaluated by noting that $\log |t|$ is constant in the range of integration. The R. H. side integral of Eq. (42) can be evaluated graphically from a knowledge of $z_1(j\omega)$.

$$\log \frac{2n}{\omega_c t_0} = \frac{2}{\pi} \int_0^{\pi/2} (\theta + \frac{\pi}{2}) \sec \nu d\nu \quad (44)$$

$$\omega_c = \frac{2n}{t_0} e^{-\frac{2}{\pi} \int_0^{\pi/2} (\theta + \frac{\pi}{2}) \sec \nu d\nu} \quad (45)$$

For ω near ω_c , $\sec \nu = 1$, and the integrand in Eq. (44) is well behaved. As ν approaches $\pi/2$, $\sec \nu$ becomes infinite so that it is necessary to determine the limit of the integrand as ω becomes infinite. At high frequencies $z_1(j\omega) \approx 0$ so that $t(j\omega)$ is determined by the load alone.

$$t(j\omega) \approx \frac{1}{1 + j\omega} = |t(j\omega)| e^{j\theta} \quad (46a)$$

$$\theta \approx -\tan^{-1} \omega \quad (46b)$$

$$\frac{\pi}{2} + \theta = \frac{1}{\omega} = \frac{1}{\omega_c \sec \nu} \quad (47)$$

Thus, at high frequencies, the integrand in Eq. (45) becomes simply $1/\omega_c$. The integrand is shown in Fig. MRI-12340-d.

To check the value of $\omega_c = 2.6$ found for $r_0 = 2$, Eq. (45) is used. $(\theta + \pi/2)$ is obtained from the empirical calculation of $\chi_1(\omega)$. Note that for the range of this integral, $r_1(\omega) = 0$ so that

$$\theta = \tan^{-1}(\omega + \chi_1(\omega)) \quad (48)$$

A curve like Fig. MRI-12340 plotted to large scale gave .677 as the value for the integral. Noting that the ideal transformer ratio required is $n = \sqrt{2}$ from (4a) and $i = n/r_0 = 1/\sqrt{2}$,

$$\omega_c = 2\sqrt{2}\sqrt{2} e^{-\frac{2}{\pi}(.677)} = 2.60 \quad (49)$$

Thus, the integral formula confirms the value $\omega_c = 2.6$ obtained from the graphical calculation. The exact agreement obtained here is probably coincidental.

It should be noted that the integral in Eq. (45) is approximately $1/\omega_c \cdot \pi/2$ which is .605 in this case, corresponding to the unshaded area of Fig. MRI-12340-d. The addition due to the shaded area is only .072. Assuming that this small contribution is approximately invariant when the $r_1(\omega)$ curve is changed, Eq. (45) can be written as

$$\omega_c e^{-\frac{1}{\omega_c}} = 4 e^{-\frac{2}{\pi}(.072)} \quad (50)$$

This is a transcendental equation whose solution from the previous calculation is known to be $\omega_c = 2.6$. The significant point here is that ω_c can be calculated even if $z_1(j\omega)$ is known only approximately.

This is a reasonable result because $\chi_1(\omega)$ for $\omega > \omega_c$ is not greatly influenced by the shape of the $r_1(\omega)$ curve in the pass band. In addition, $\chi_1(\omega)$ is small compared to the parasitic reactance of the load for large ω . This makes $(\theta(\omega) + \pi/2)$ for $\omega > \omega_c$ practically independent of the exact form of $z_1(j\omega)$. However, $(\theta + \pi/2)$ is a function of ω , while the integral is expressed in terms of ω/ω_c . This process of normalization makes the integrand almost inversely proportional to ω_c .

6. Performance of Series-L Matching Network

The $I(\omega)$ curve for the last locus of Fig. MRI-12137 is shown in Fig. MRI-12138. It is compared with the curve obtained by making $z_1(p)$ a simple R-C circuit as shown in the figure.

It can be seen that the bandwidth of the complicated empirical design is about 1.5 times the bandwidth of the simple R-C circuit.

D. The Shunt-L Matching Network

There is no a priori reason why an L-pad consisting of a shunt element followed by a series element should be better than an L-pad with series and shunt elements occurring in the opposite order. The use of the matching network of Fig. MRI-12300-b will therefore be considered in this section. For this network:

$$P(\omega) = \frac{|y(j\omega)|^2}{n^2 |y_2(j\omega)|^2} \quad (51)$$

For $P(\omega) = P_0$ in the "pass band" it is necessary to make

$$|y_2(j\omega)| = \frac{1}{n \sqrt{P_0}} |y(j\omega)| \quad 0 \leq \omega \leq \omega_c \quad (52)$$

$y(j\omega)$ is given as $\frac{1}{1 + j\omega}$, so if values are chosen for n and P_0 , for each ω there is a circle centered about the origin of the admittance plane whose radius is $\frac{|y(j\omega)|}{n \sqrt{P_0}}$ (referred to as an " ω -circle".) A

point on the $y_2(j\omega)$ locus corresponding to any value of ω must fall on the appropriate ω -circle. Some critical ω -circles are shown in MRI-12303. In addition, the y_2 locus can intersect only a certain portion of each circle: that part of the circle which lies to the right of the point representing $y(j\omega)$ in the admittance plane. In other words, $g_2(\omega) \geq g(\omega)$. This restriction is necessary to insure that $g_1(\omega) \geq 0$.

Note that in the previous section a locus had to be designed which followed a single curve: a circular arc for $0 < \omega < \omega_c$ and a straight line for $\omega > \omega_c$. The present problem specified a different curve for each ω for $0 < \omega \leq \omega_c$ and then specifies nothing at all for $\omega > \omega_c$ (except that $g_2(\omega) \geq g(\omega)$). The latter problem might seem to be more difficult because of the greater complexity in the specification of the desired locus.

In the present case, however, the locus specification does not introduce undue difficulties. Actual trial shows that the desired locus intersects many of the ω -circles near the axis abscissas. The ω -circle arcs are normal to this axis so that the susceptance may vary to a considerable extent without requiring an appreciable change in conductance in order to remain on the proper ω -circle. This means that the points at which the ω -circles cross the real axis give a good initial guess for the conductance function.

An additional requirement on the $y_2(j\omega)$ locus of this problem is that $R_2(\omega) < n^2$ to permit physical realizability of z_3 . This means that the $y_2(j\omega)$ locus must not intersect the "transformer-setting" circle of Fig. MRI-12301-a. This circle, as described in the preceding section, is the admittance-plane map of $r_2 = n^2$. The problem is now to find a $y_2(j\omega)$ which satisfied the above requirements and makes ω_c as large as possible. Two alternatives exist:

(1) y_1 is a minimum susceptance function. The $y_2(j\omega)$ locus touches the transformer-setting circle at $\omega = \omega_c$ and follows it for $\omega_c \leq \omega < \infty$ as shown in Fig. MRI-12301-b.

(2) y_1 is not a minimum susceptance function: it has some shunt capacitance. This permits the $y_2(j\omega)$ locus to run over the top of the transformer-setting circle in the manner of Fig. MRI-12301-c. It is tangent to the circle at some ω in the pass band.

The conductance curves for the two alternatives are shown in Fig. MRI-12302-a. For alternate (1) the $g_2(\omega)$ curve dips down and then rises to the value of $\frac{1}{n^2}$ while for alternate (2) the $g_2(\omega)$ curve keeps dropping until it reaches the $g(\omega)$ curve. The $g_2(\omega)$ curve cannot be controlled beyond this point because there is no more conductance left in $g_1(\omega)$ to be removed. ω_c is that value of ω at which the $g_2(\omega)$ curve reaches the $g(\omega)$ curve.

In alternate (1) note that the $y_2(j\omega)$ locus runs into the transformer-setting circle at a value of $|y_2|$ slightly smaller than $\frac{1}{n^2}$.

$$|y_2(j\omega_c)| \approx \frac{1}{n^2} \quad (53)$$

As long as $\frac{1}{n^2} - |y_2(j\omega)|$ is small, Eq. (53) can be substituted in Eq. (52) giving

$$\sqrt{P_o} = n |y(j\omega_c)| \quad (54)$$

From this it can be seen that for a given ω_c , the largest possible n should be chosen to make P_o a maximum. The upper limit on n can be found by considering the network at $\omega = 0$, where it is entirely resistive. In Fig. MRI-12300-c, the largest value of n for a given P_o is obtained by making $g_1(0) = 0$ so that

$$\sqrt{P_o} = \frac{n}{1 + r_3(0)} = \frac{n}{n^2} = \frac{1}{n} \text{ giving}$$

$$\text{maximum allowable } n = \frac{1}{\sqrt{P_o}} \quad (55)$$

With this value of n , Eq. (52) requires that

$$|y_2(j\omega)| = |y(j\omega)| \quad (56)$$

This alternative was worked out in detail for $P_o = \frac{1}{2}$ and the $y_2(j\omega)$ locus is shown in Fig. MRI-12303. The value of ω_c obtained is 1.8, quite a bit less than the $\omega_c = 2.6$ obtained for the network of Fig. MRI-12300-a. Note that the approximate ω_c given by Eq. (54) is $\sqrt{3}$ which is in error by less than 5%.

The best value of n for alternate (2) is not so obvious. A value of n less than the maximum value allows a larger range of $g_1(\omega)$ variation which would be an advantage if the $y_2(j\omega)$ locus did not have to be maneuvered around the transformer-setting circle. The diameter of

this circle varies as $\frac{1}{n}$ so that the increase in size of this circle is more rapid than the increase in range of $g_1(\omega)$. As n is decreased, a larger shunt capacitance must be used in y_1 and $g_1(\omega)$ must fall off faster in order to intersect the proper circles for each ω . As n is decreased from its maximum permissible value of $\frac{1}{\sqrt{P_0}}$ it is actually found by trial that ω_c becomes smaller because the increase range of $g_1(\omega)$ is more than offset by the difficulty of getting the y_2 locus around the larger transformer-setting circle. Thus, the best value for n turns out to be the largest permissible value.

Alternate (2) is worked out for $P_0 = \frac{1}{2}$ and the y_2 locus is shown in Fig. MRI-12303. The $\omega_c = 2.4$ obtained in this design is better than the $\omega_c = 1.8$ for alternate (1) but is not as good as the $\omega_c = 2.6$ obtained for the series L-pad of Fig. MRI-12300-a.

E. A T-pad Matching Network

It might occur to an investigator that for the simple load $z = 1 + p$, no advantage is obtained by using more complex matching configurations than the series and shunt structures so far considered. This conclusion is encouraged by the difficulty of designing a more complicated structure to give a greater ω_c for the same P_0 . One such network, however, has been designed and is reported here to indicate that more complicated networks can give better performance than the best of the T-pads.

For the ideal transformer and T-pads of Fig. MRI-12300-d,

$$R(\omega) = \frac{|y_2(j\omega)|}{n^2 |y_4(j\omega)|^2} \quad (57)$$

Physical realizability of the elements of the T requires

$$r_2(\omega) \geq r(\omega), \quad g_4(\omega) \geq g_2(\omega), \quad r_4(\omega) \leq n^2 \quad (58)$$

The $z_1(j\omega)$ function is arbitrarily picked as a low pass filter function which is similar to the result obtained for z_1 in the series matching case (Fig. MRI-12300-a).

$$z_1(j\omega) = r_1(\omega) + jx_1(\omega) = \sqrt{1 - \left(\frac{\omega}{\omega_c}\right)^2} - j \frac{\omega}{\omega_c} \text{ for } 0 \leq \omega \leq \omega_c \quad (59a)$$

$$r_1(\omega) = 0 \text{ for } \omega_c \leq \omega < \infty \quad (59b)$$

y_2 is known and is plotted in Fig. MRI-12304 for $\omega_c = \sqrt{3} + 1 = 2.732$. For $P(\omega) = P_0$ in the pass band:

$$|y_1(j\omega)| = \frac{1}{n\sqrt{P_0}} |y_2(j\omega)| \quad 0 \leq \omega \leq \omega_c \quad (60)$$

The realizability requirements Eq. (58) require that the $y_1(j\omega)$ locus should stay outside of the transformer-setting circle and that every point of $y_1(j\omega)$ should be directly above or to the right of the corresponding point on $y_2(j\omega)$. This is easily accomplished by a y_3 which contains a shunt condenser. The $y_1(j\omega)$ locus is plotted in Fig. MRI-12304 for $P_0 = \frac{1}{2}$ and $n = \sqrt{2}$. The associated $g_1(\omega)$ curve is shown in Fig. MRI-12302-b.

The $\omega_c = 2.73$ obtained here is only slightly better than the $\omega_c = 2.6$ obtained for the best of the L-pads, but the ease with which this network was designed seems to indicate that considerable improvement in performance may be obtained by designing the optimum T network and points towards the use of even more general networks.

IV. Comparison of Various Matching Networks

All the empirical designs of sections III B, C, and D were worked out for $P_0 = \frac{1}{2}$. It is instructive to compare the performance of the L and T pad networks with the complementary filter matching networks of Part III-B. Such a comparison will give an indication of how much bandwidth is obtained by eliminating the ripples associated with the complementary filter design. The Butterworth characteristic for large n was not found to be satisfactory so the examples selected from III B are the Tschbycheff filter for large n and the response for $n = 1$. (For this value of n , the Butterworth and Tchebycheff functions are identical.) The basis for comparison will be the value of ω_c obtained with each network for $L_0 = 1$ and $\frac{1}{P} \leq P(\omega) \leq 1$ for $0 \leq \omega \leq \omega_c$. To do this, it is

merely necessary to set $\epsilon = 1$ so that $\frac{1}{1 + \epsilon^2} = \frac{1}{2}$. The value of L_0 obtained for the large n Tschebycheff filter is the value of ω_c which would have been obtained if ω_c had not been set equal to 1 and L_0 were fixed at 1. The results are tabulated below:

Comparison & Matching
 Section Performance

Section, Type	Max. P(ω)	Min P(ω) $0 \leq \omega \leq \omega_c$	ω_c
A. $n = 1$ (Butterworth or Tschebycheff)	1	1/2	1
A. Tschebycheff $n \rightarrow \infty$	1	1/2	1.78
B. L-pad	1/2	1/2	2.6
C. L-pad Alternate 1	1/2	1/2	1.8
C. L-pad Alternate 2	1/2	1/2	2.4
D. T-pad	1/2	1/2	2.73

RESTRICTED

Report R-264-52, PIB-203
Contract No. N0bsr-43360
Index No. NE-100-402

R1

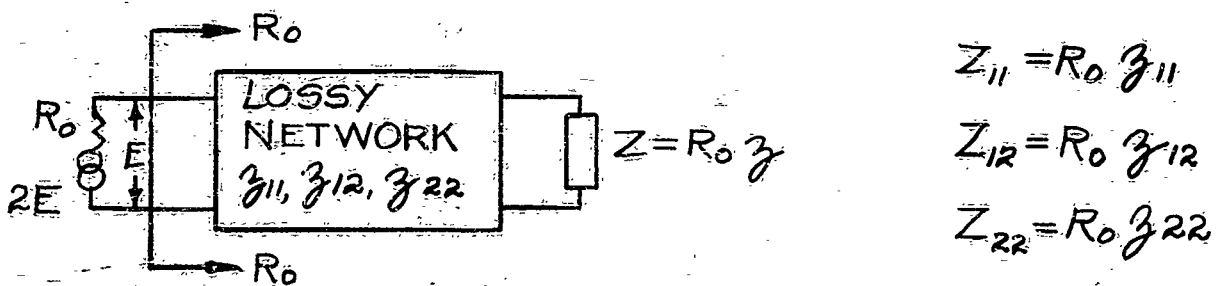
REFERENCES

1. R. M. Fano, "Theoretical Limitations on the Broadband Matching of Arbitrary Impedances", Jour. Franklin Institute, v. 249, n. 1 Jan. 1950.
2. H. W. Bode, "Network Analysis and Feedback Amplifier Design", New York, D. Van Nostrand Co., 1945, p. 199.
3. Bode, loc. cit., p. 364.
4. S. Darlington, "Synthesis of Reactance n -Poles", Journal of Mathematics and Physics, M.I.T., v. 28, n. 4, Sept. 1939.
5. E. L. Norton, "Constant Resistance Networks with Applications to Filter Groups", Bell System Technical Journal, v. 16, pp. 178-193, April 1937.
6. H. W. Bode, "A Method of Impedance Correction", Bell System Technical Journal, v. 9, pp. 794-835, Oct., 1930.
7. H. W. Bode, "Network Analysis and Feedback Amplifier Design", New York, D. Van Nostrand Co., 1945, p. 297.

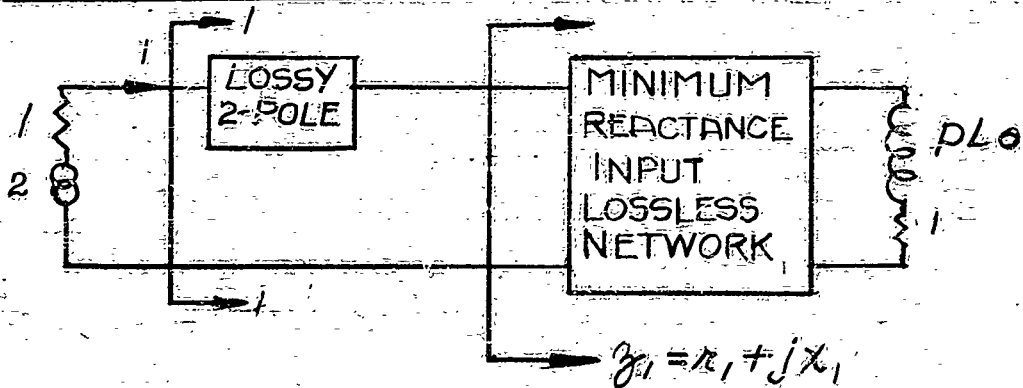
RESTRICTED

RESTRICTED

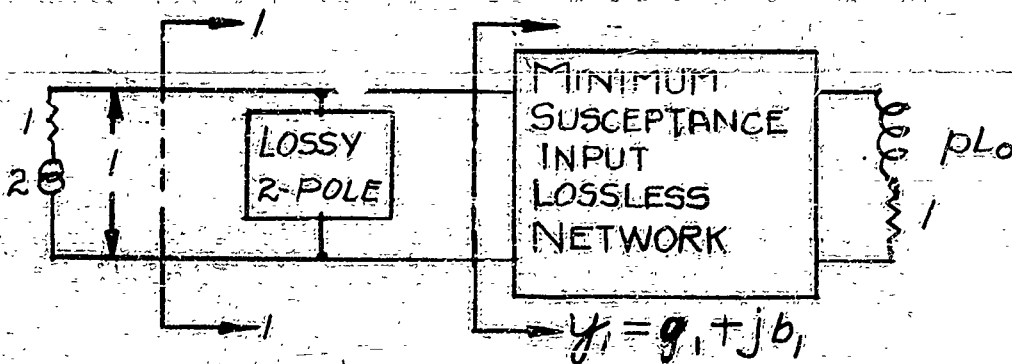
MATCHING NETWORKS



(a) GENERAL MATCHING NETWORK

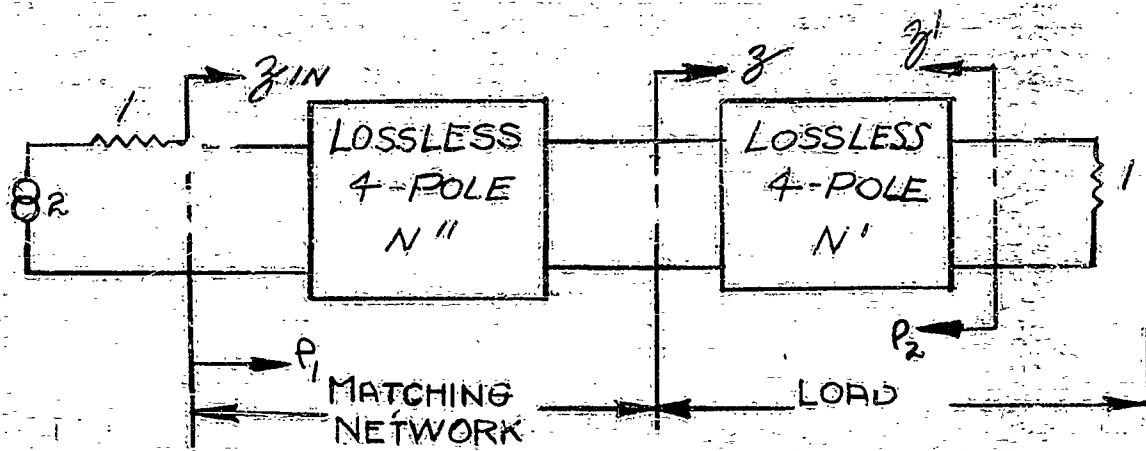


(b) SPECIAL MATCHING STRUCTURE

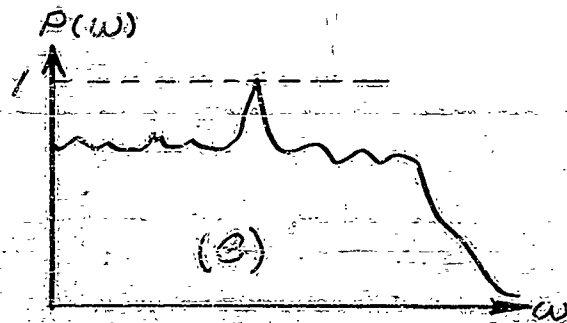
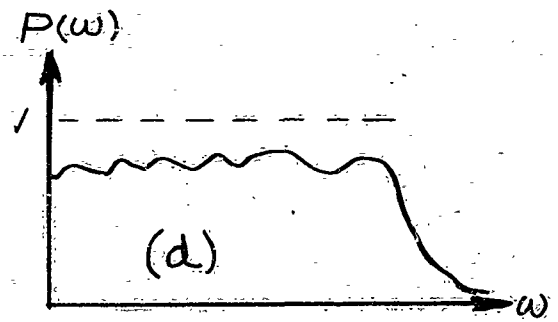
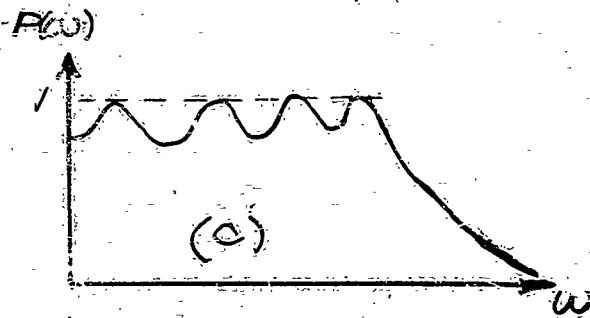
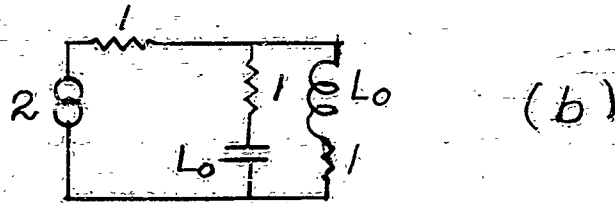


(c) SPECIAL MATCHING STRUCTURE

RESTRICTED



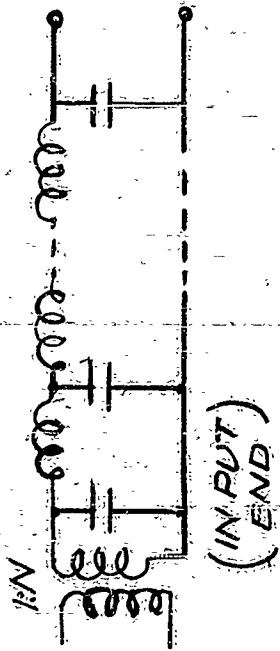
(a) LOSSLESS MATCHING STRUCTURE



MATCHING NETWORKS & $P(\omega)$ CURVES

RESTRICTED

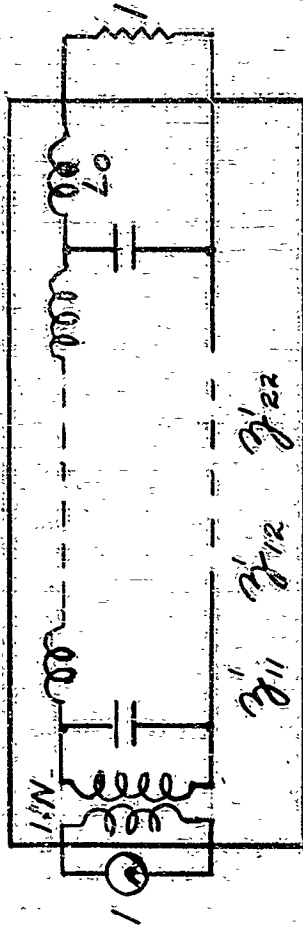
TRANSFORMATION OF LOSSLESS LADDER TO INCLUDE LOAD REACTANCE



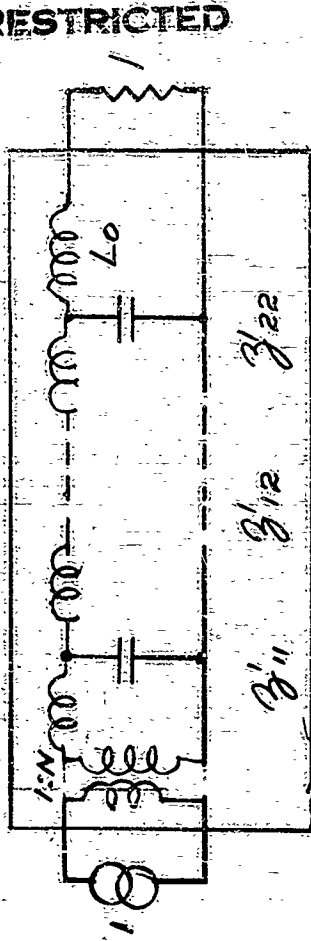
(a) MINIMUM REACTANCE INPUT LOSSLESS LOW-PASS LADDER



(b) MINIMUM SUSCEPTANCE INPUT LOSSLESS LOW PASS LADDER



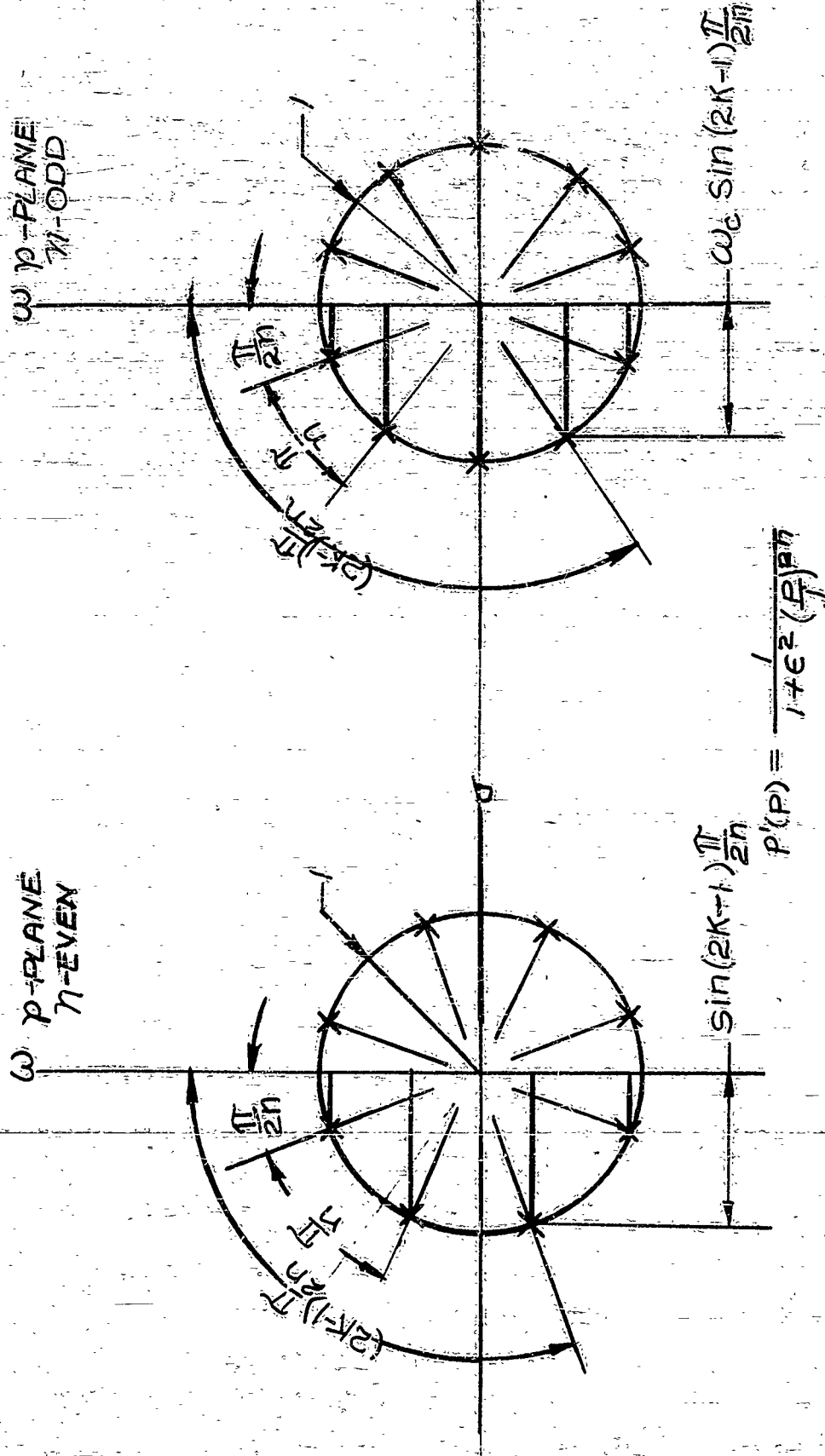
(c) EQUIVALENT NETWORK FOR POWER CALCULATIONS



(d) EQUIVALENT NETWORK FOR POWER CALCULATIONS

RESTRICTED

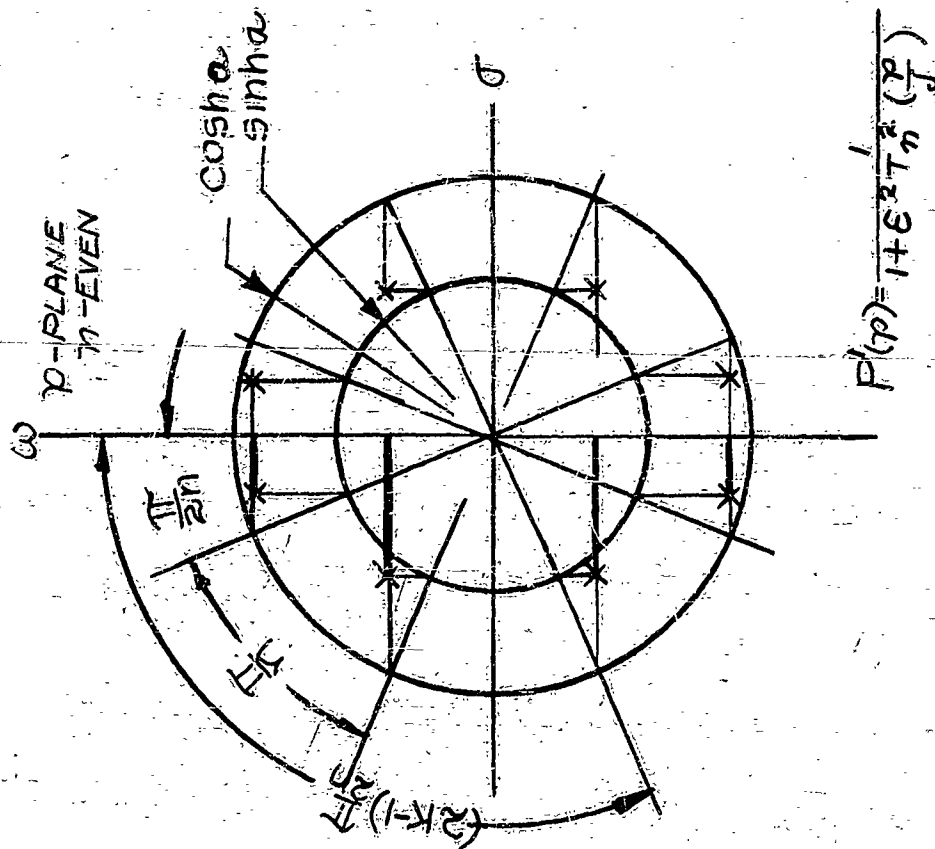
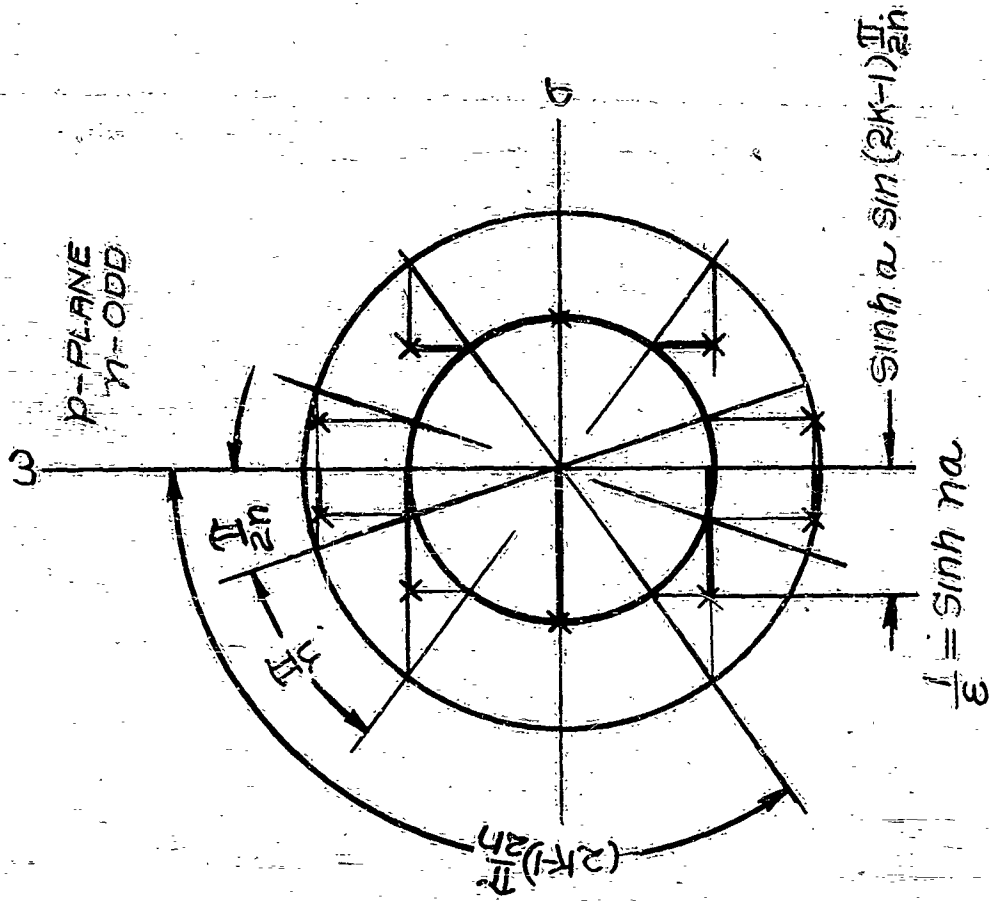
RESTRICTED



RESTRICTED

POLES OF BUTTERWORTH TYPE APPROXIMATING FUNCTION

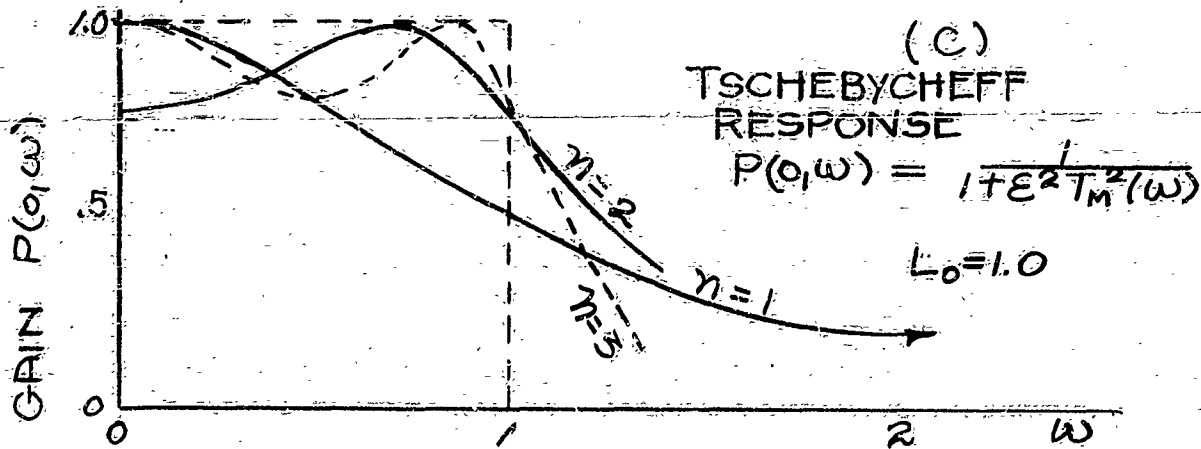
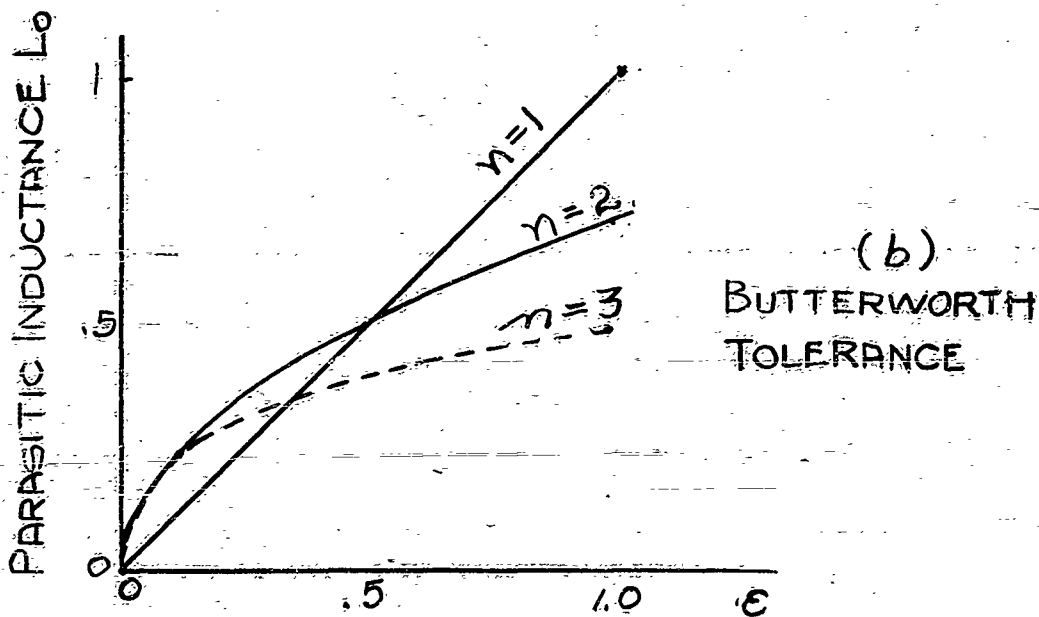
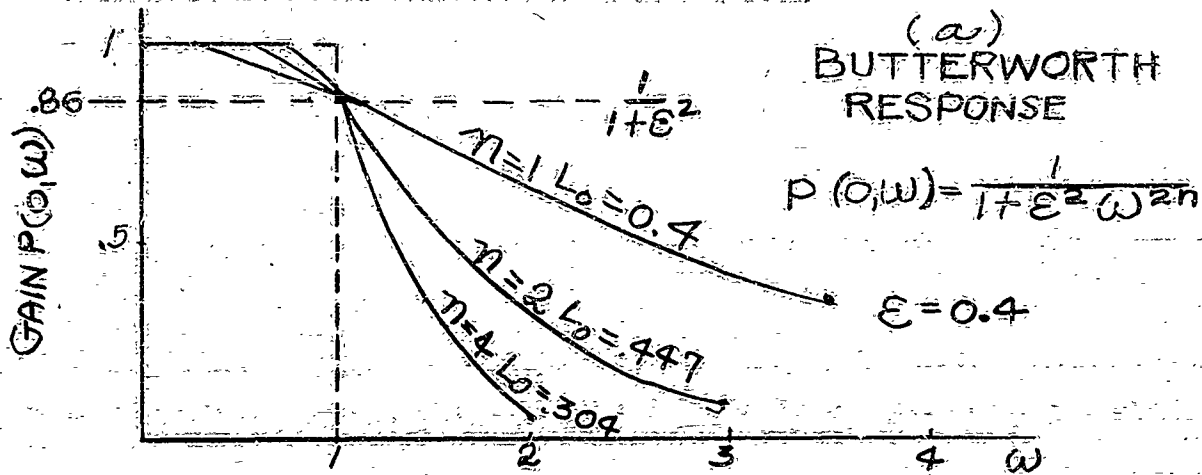
RESTRICTED



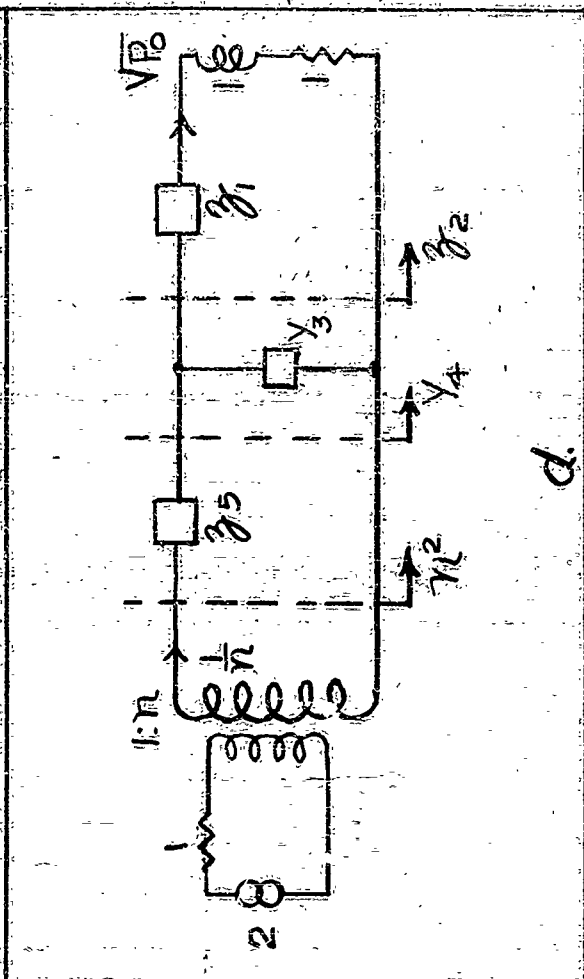
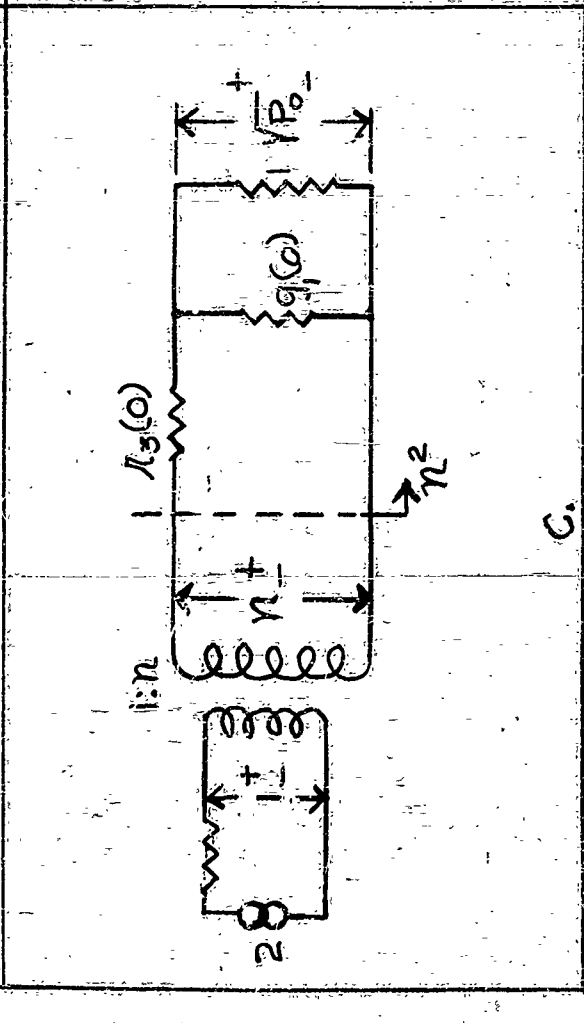
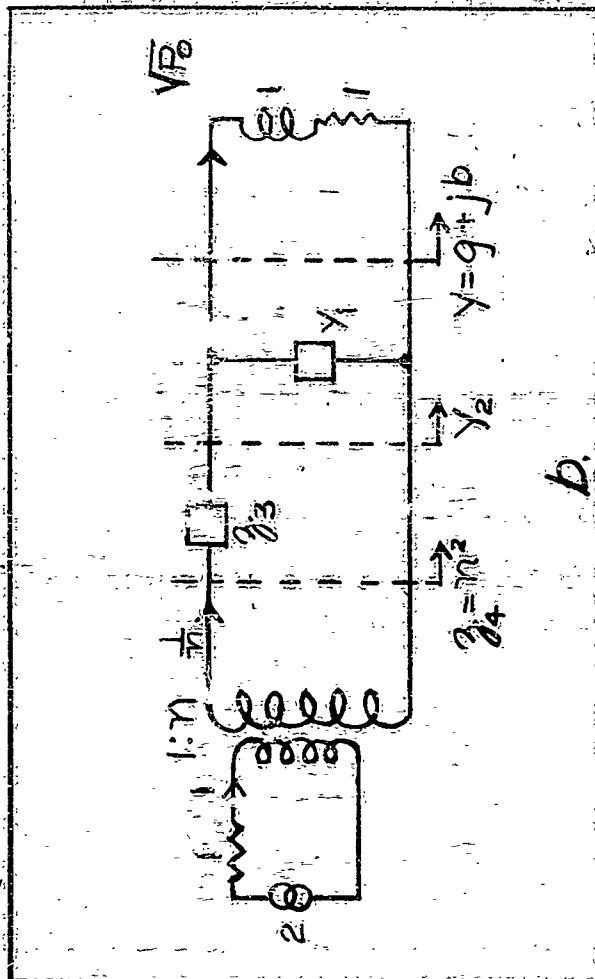
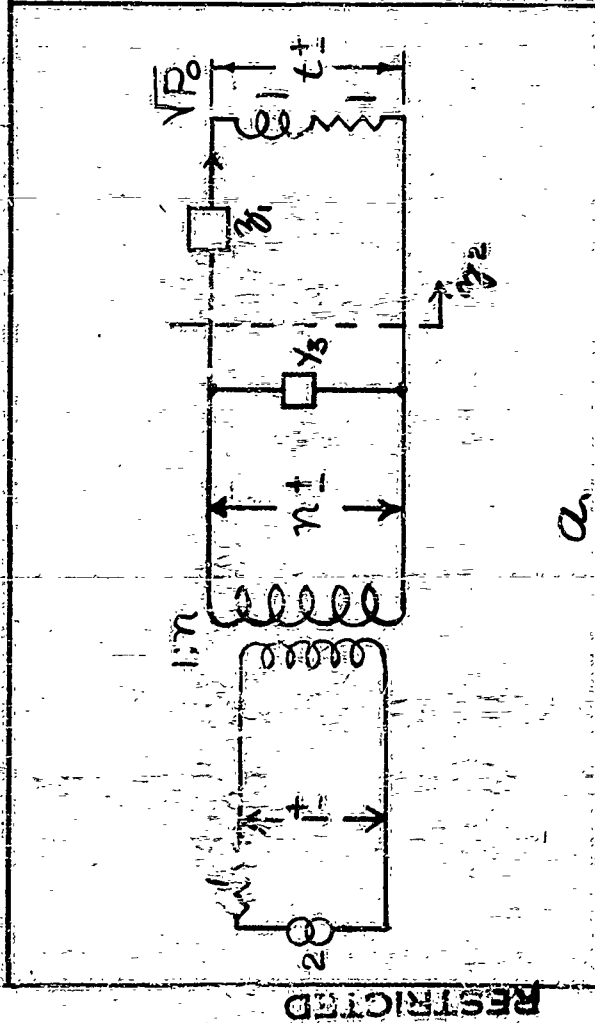
POLES OF TSCHEBYCHEFF TYPE APPROXIMATING FUNCTION

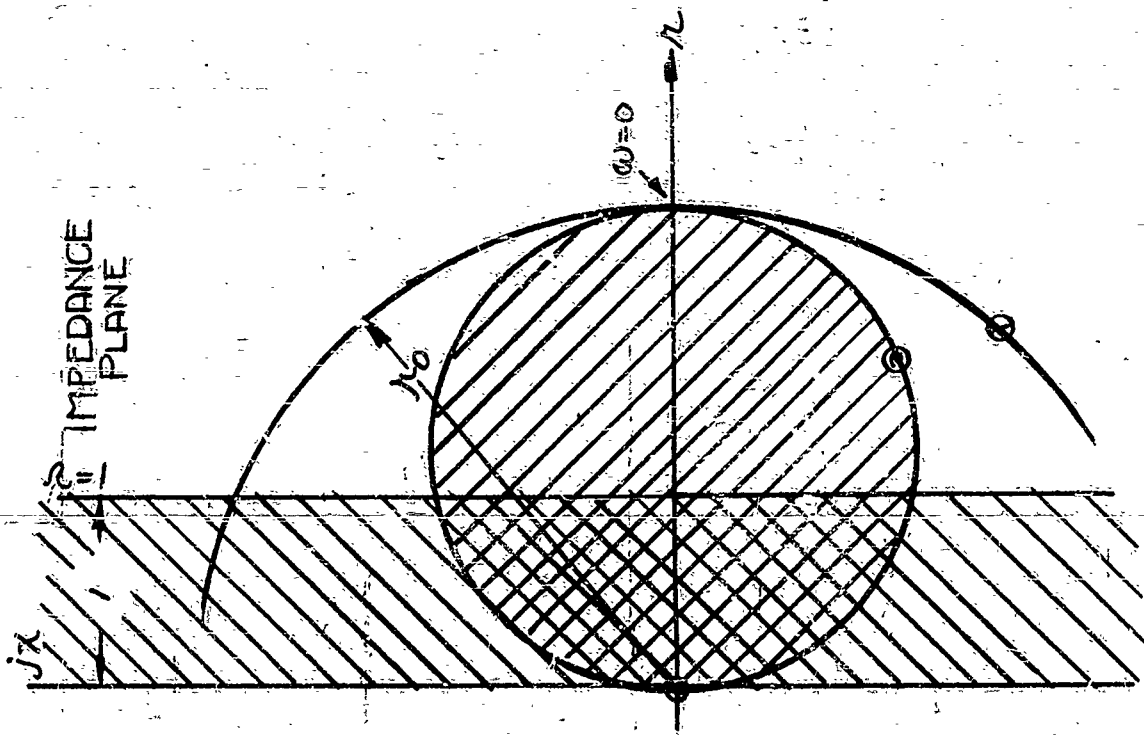
M.R.I-11971

GAIN & TOLERANCE CURVES

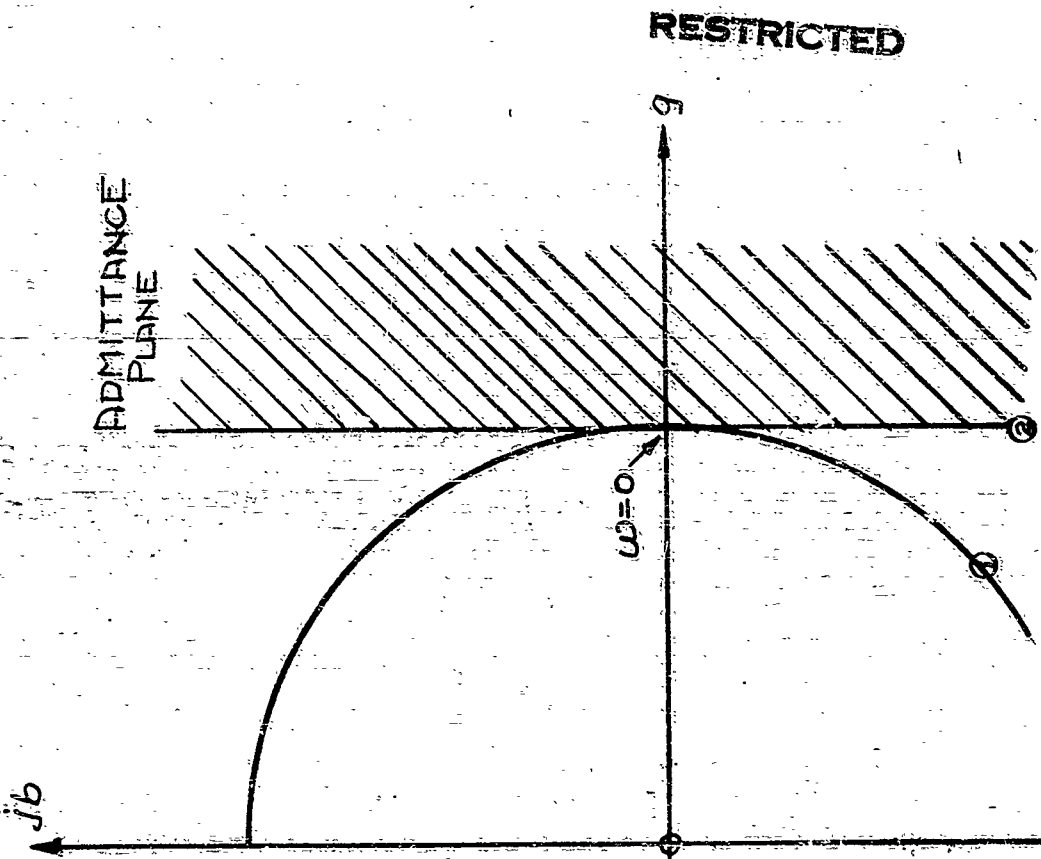


SIMPLE MATCHING NETWORKS





RESTRICTED

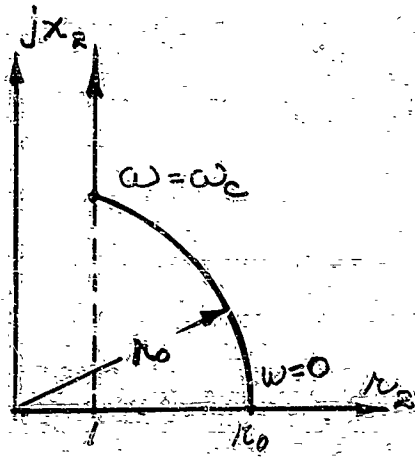


ADMITTANCE
PLANE

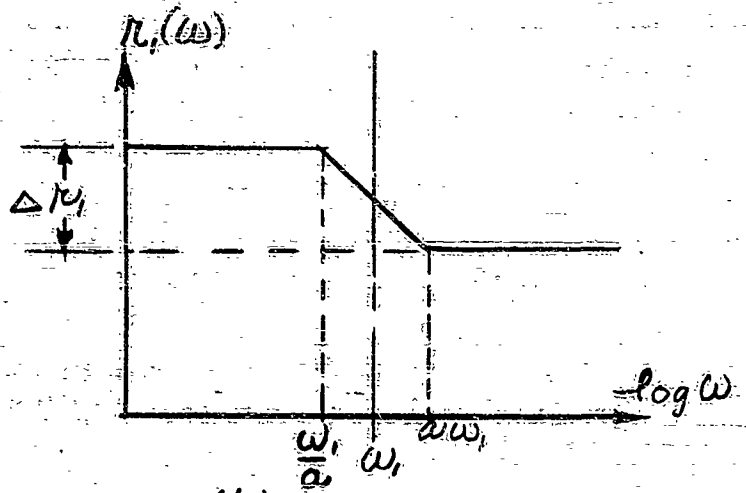
RESTRICTED

RESTRICTED REGIONS OF IMPEDANCE AND ADMITTANCE PLANES

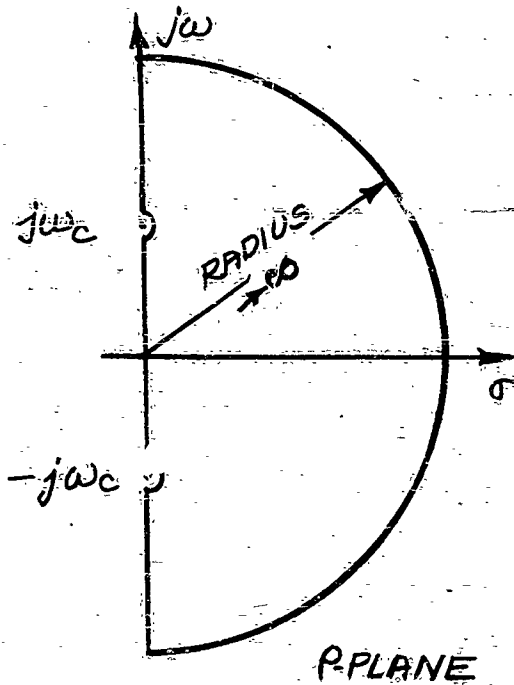
RESTRICTED



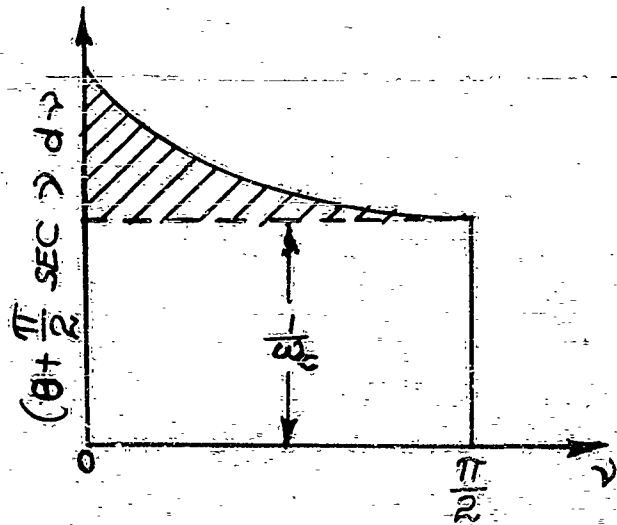
(a)



(b)



(c)

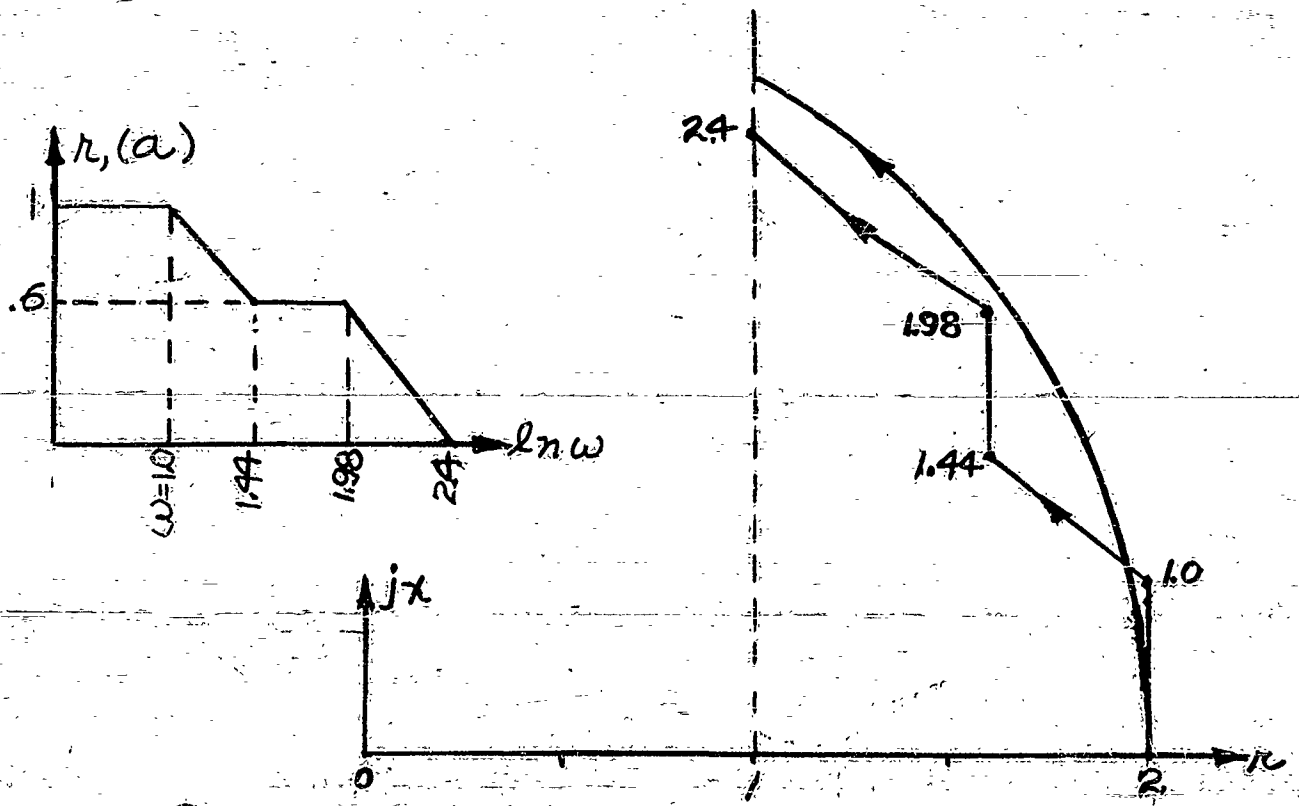
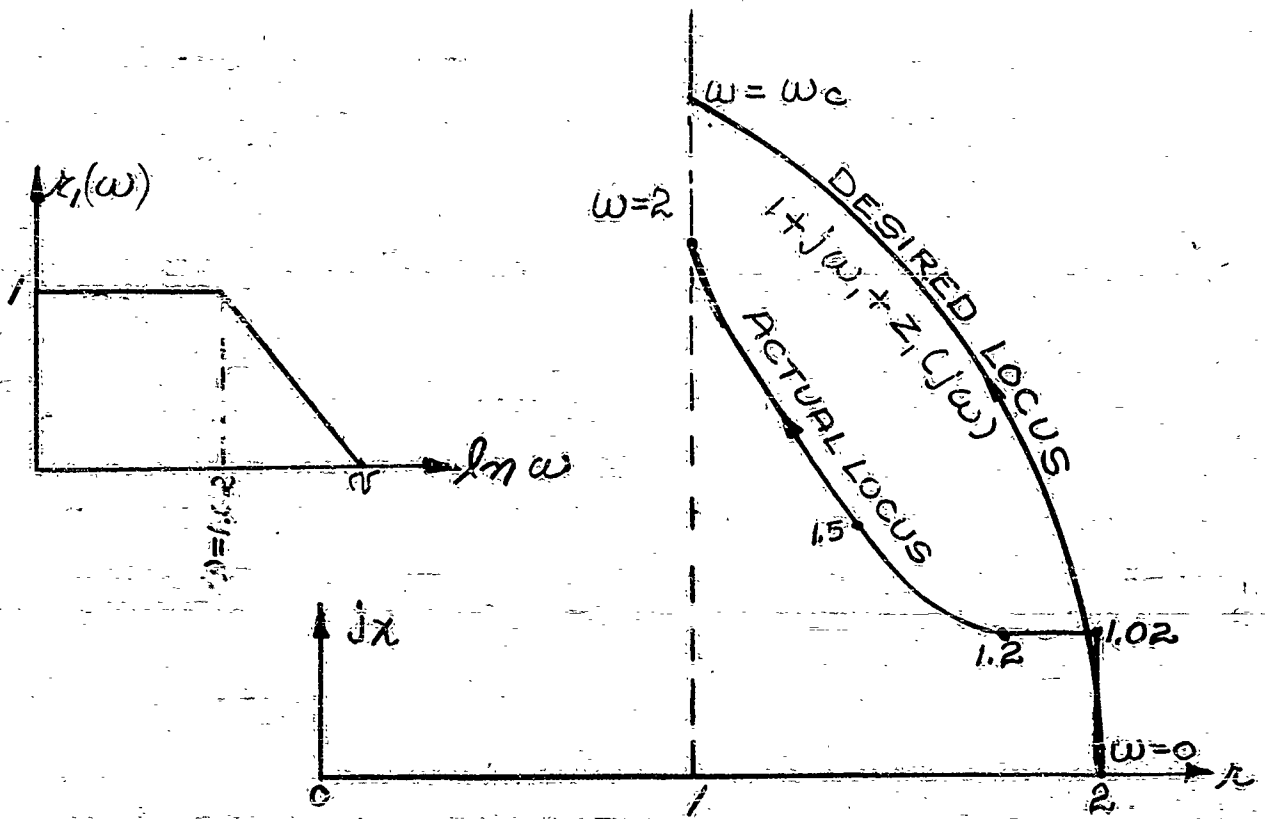


(d)

IDEAL IMPEDANCE LOCUS, FINITE LINE SEGMENT,
P-PLANE PATH, PHASE SHIFT INTEGRAND

RESTRICTED

RESTRICTED

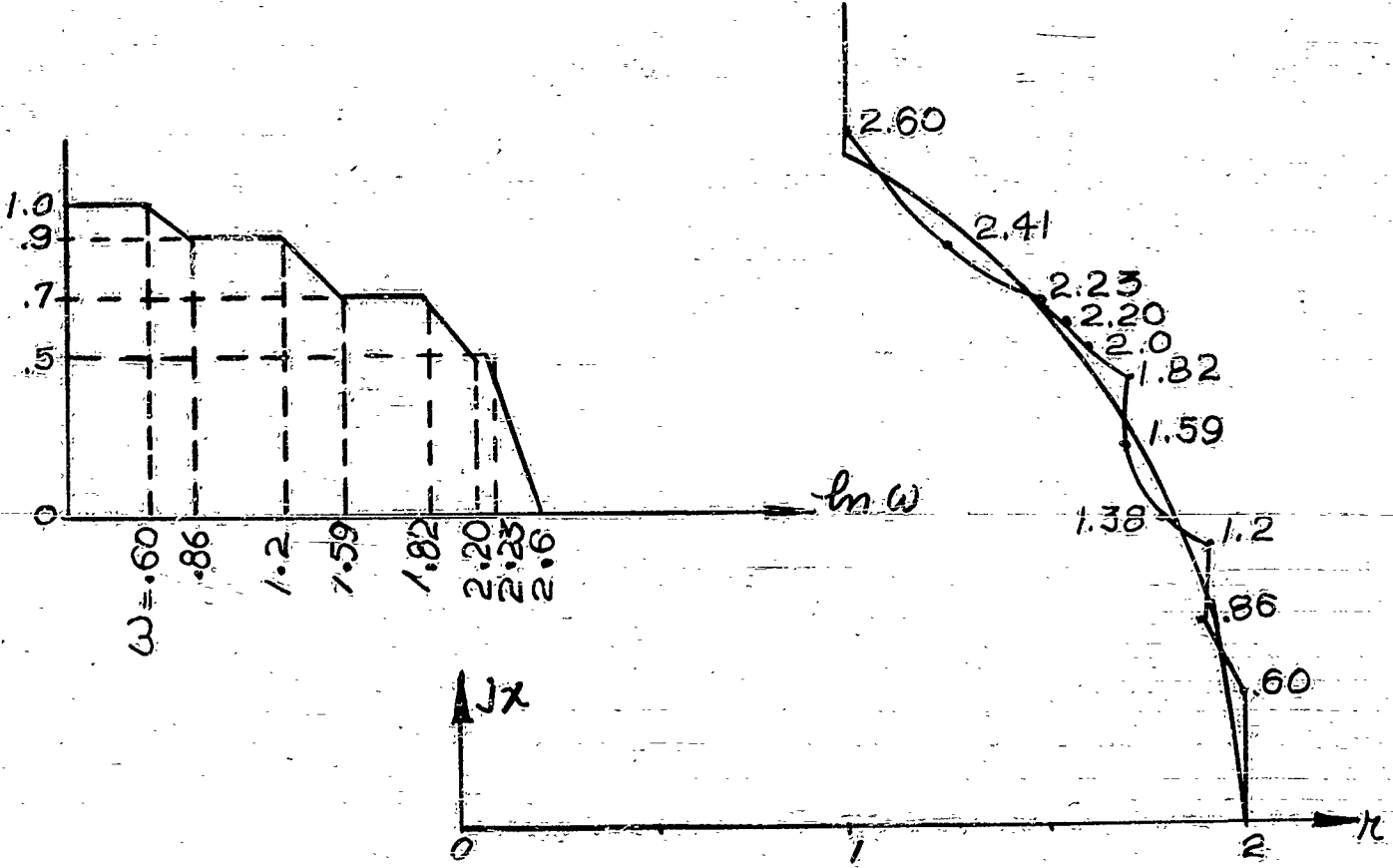
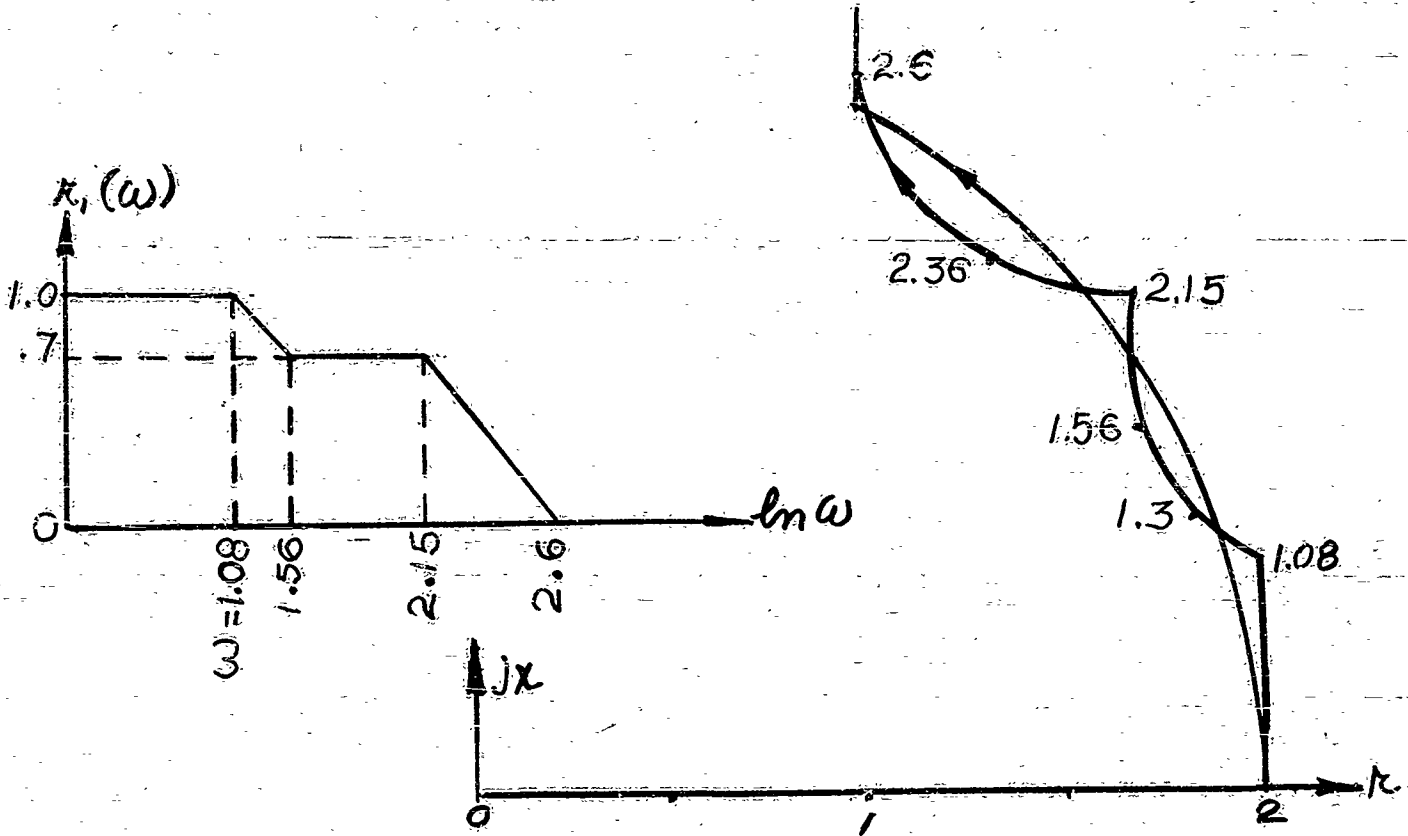


CALCULATED LOCI

RESTRICTED

MR.1-12136

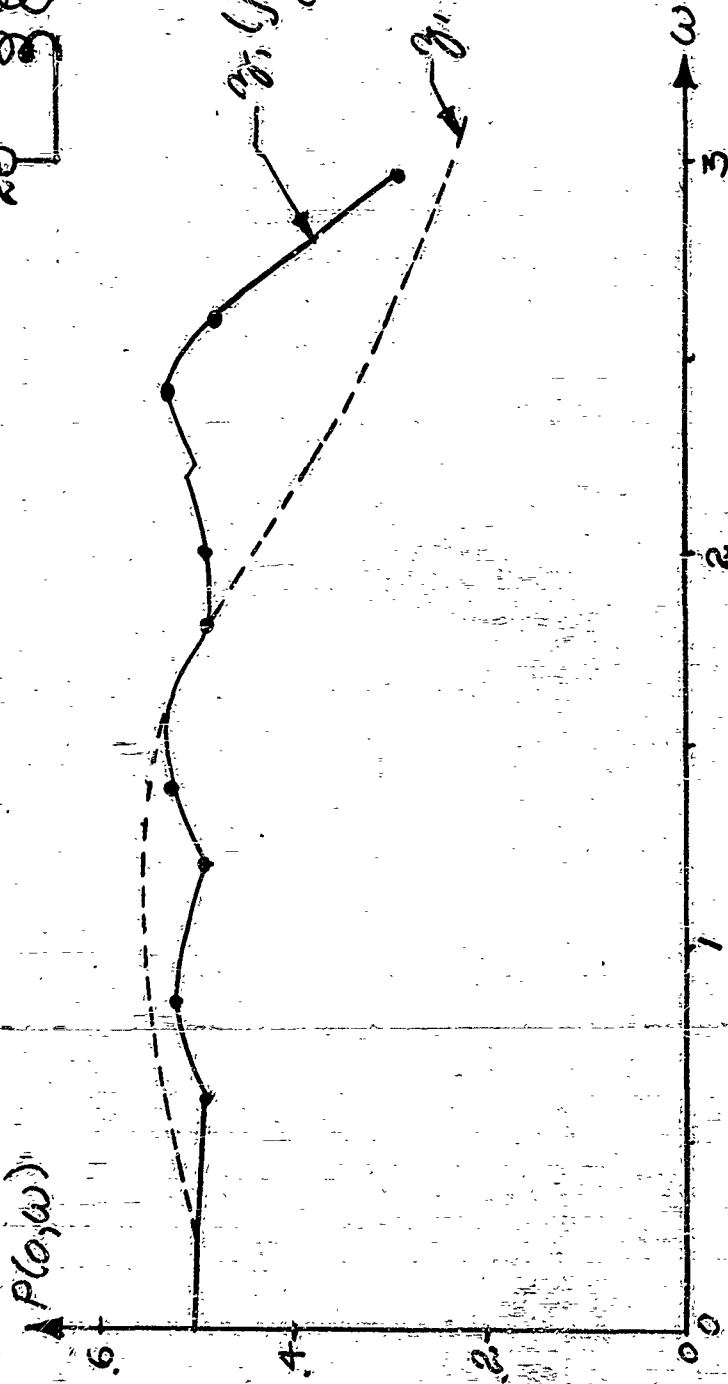
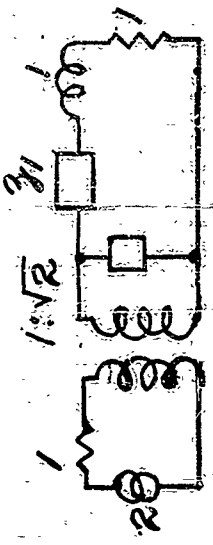
RESTRICTED



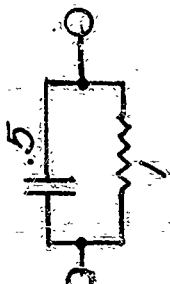
CALCULATED LOCI

RESTRICTED

RESTRICTED



$z_1(j\omega)$ PICKED FOR
OPTIMUM RESPONSE



$z_1(p) =$

PERFORMANCE OF CALCULATED NETWORK

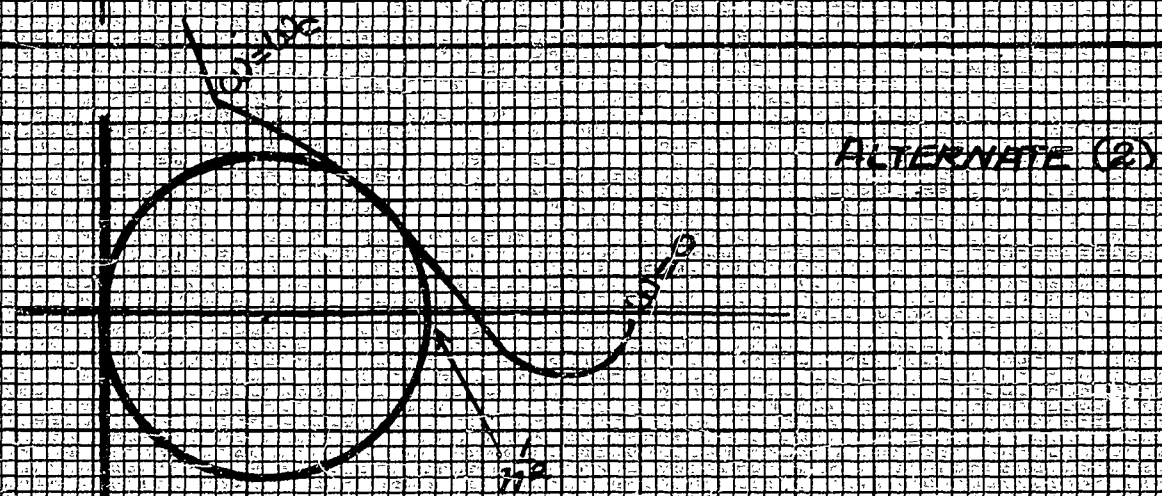
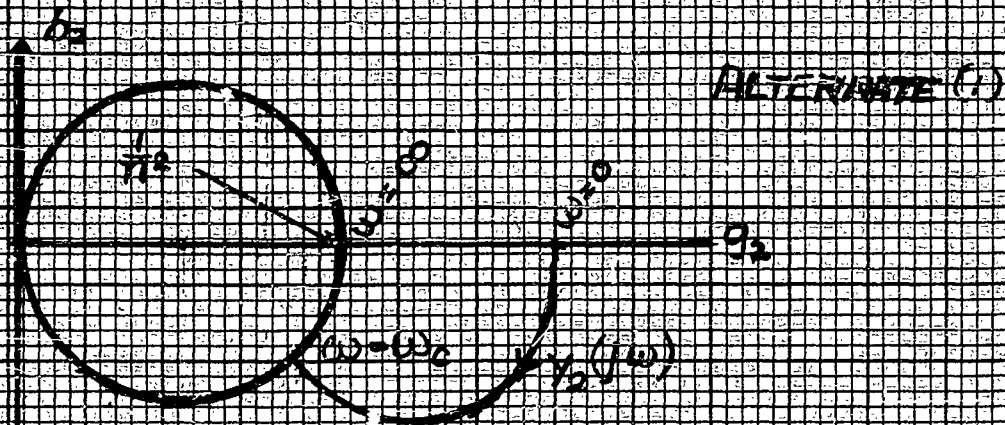
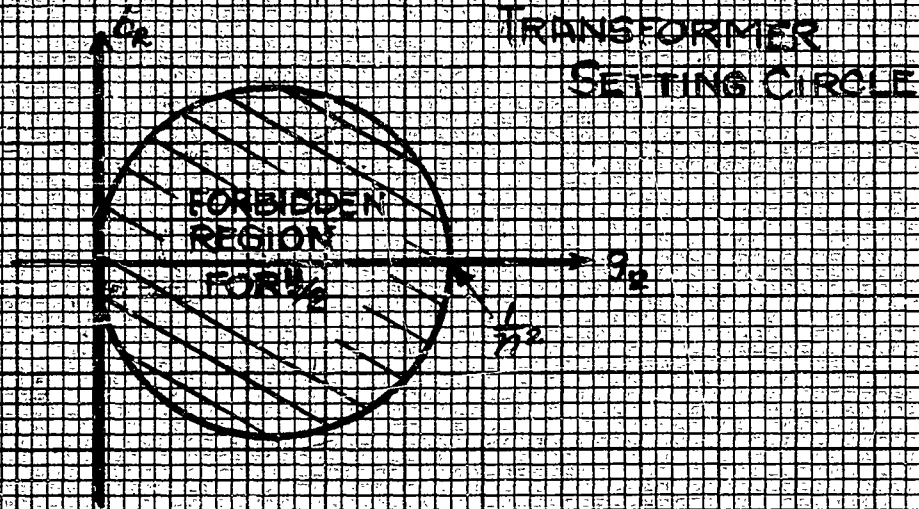
M.R. 1-12/38

8-51

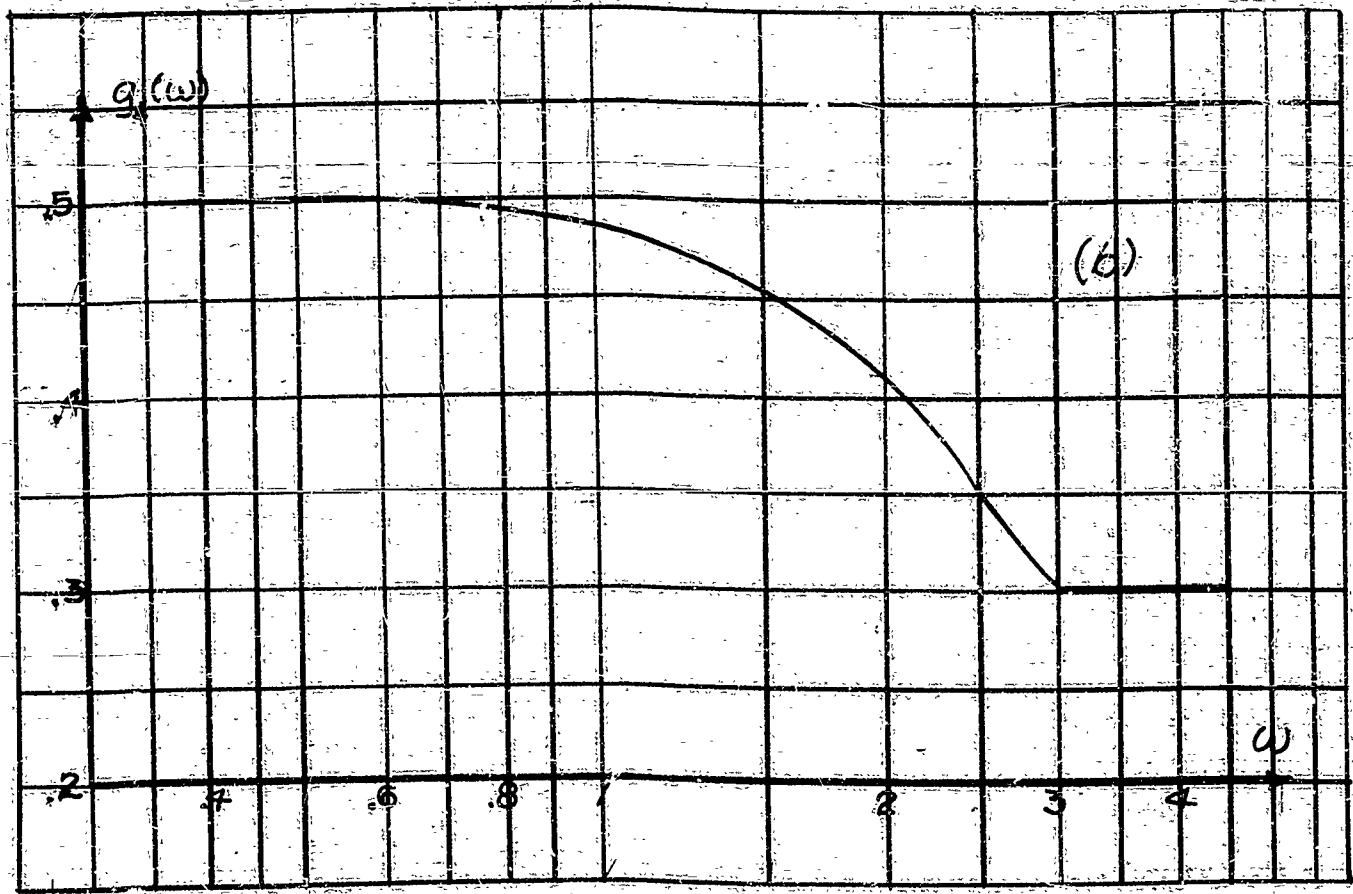
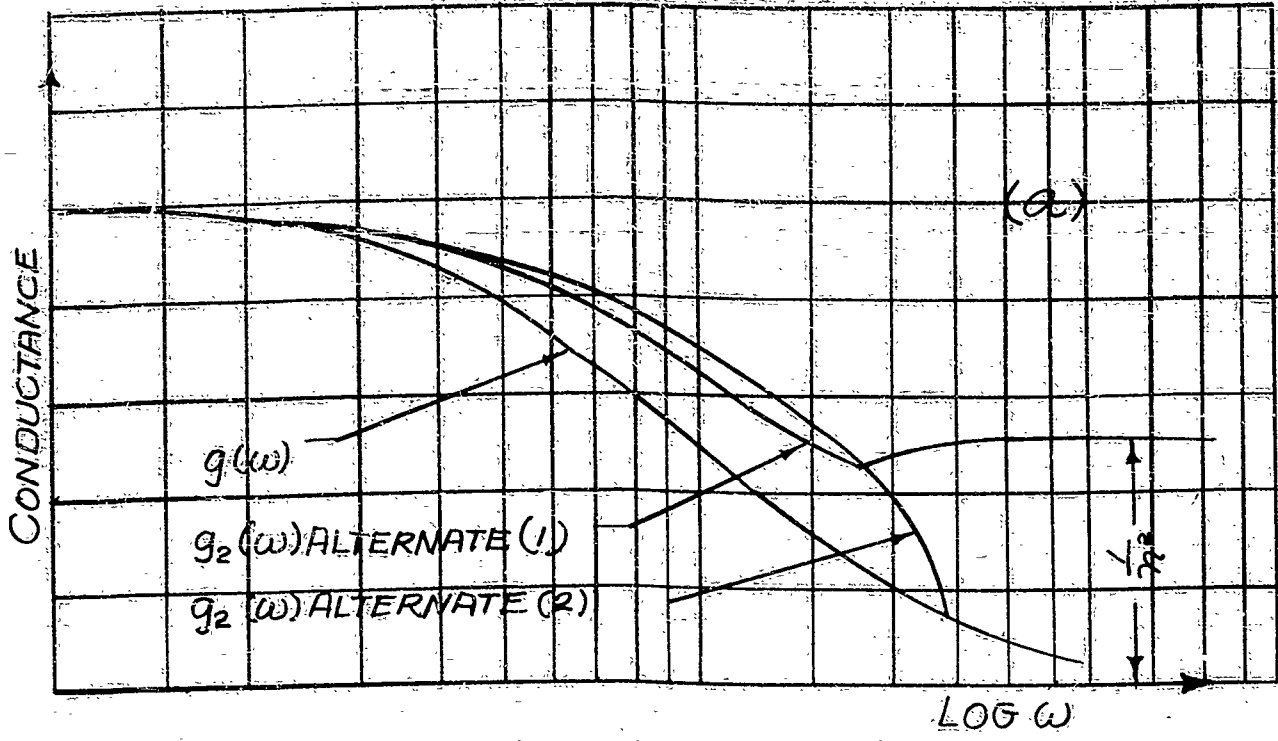
RESTRICTED

RESTRICTED

X_2 PLANES

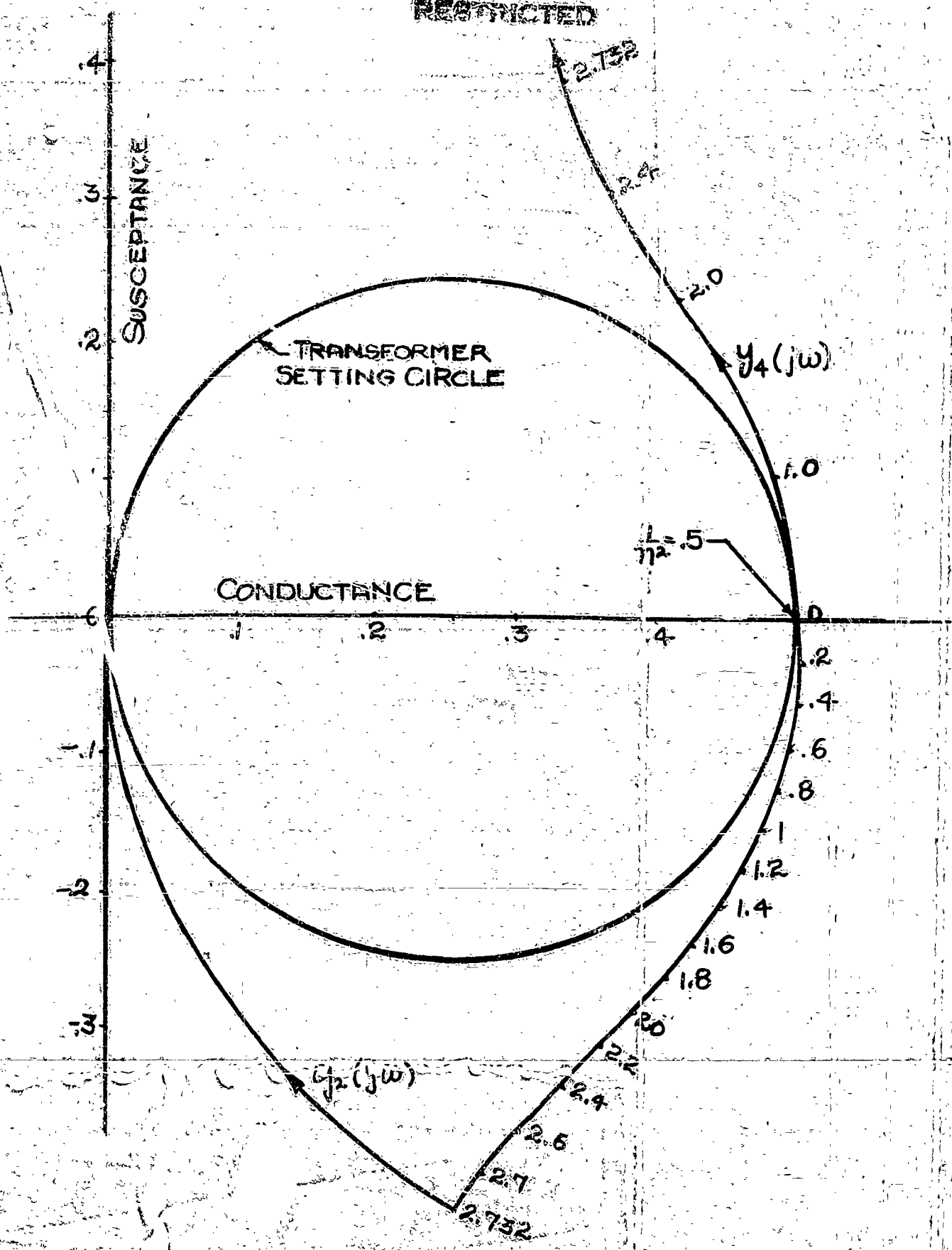


RESTRICTED



CONDUCTANCE CURVES

RESTRICTED



ADMITTANCE LOCI FOR T-SECTION

11-51

M.R.I-12304

RESTRICTED

STI-ATI-205 300

RESTRICTED

Microwave Research Inst., Polytechnic Inst. of
Brooklyn, N.Y.

A CLASS OF BROAD-BAND DISSIPATIVE MATCHING NETWORKS DESIGNED ON AN INSERTION-LOSS BASIS, by
Richard LaRosa and Herbert J. Carlin. 25 Jan 52, 26p
illus, tables. Rept no. R-264-52, PIB-203. Contract
NObsr-43360

Electronics & Electronic
Equipment (8)
Electronic Theory (3)

Networks - Insertion loss

(Copies obtainable from ASTIA-DSC)

MICROFILMED

RESTRICTED